Molecular Pharmacology Fast Forward. Published on September 1, 2011 as doi: 10.1124/mol.111.074302
This article has not been copyedited and formatted. The final version may differ from this version.

MOL #74302

Title page

Investigation of the molecular mechanism of the alpha7 nAChR positive allosteric modulator PNU-120596 provides evidence for two distinct desensitized states

Dustin K. Williams, Jingyi Wang, and Roger L. Papke

Dept. of Pharmacology and Therapeutics, University of Florida, College of Medicine, Gainesville, Florida, USA (DKW, RLP)

Dept. of Chemistry, University of Florida, Gainesville, Florida, USA (JW)

Molecular Pharmacology Fast Forward. Published on September 1, 2011 as DOI: 10.1124/mol.111.074302
This article has not been copyedited and formatted. The final version may differ from this version.

Running Title page

Running title: Modulation of α7 nAChR

*To whom correspondence should be addressed:

Name: Roger L. Papke

Phone: 352-392-4712

Fax: 352-392-9696

E-mail: rlpapke@ufl.edu

Address: Department of Pharmacology and Therapeutics

University of Florida

P.O. Box 100267

Gainesville, FL 32610-0267

Number of text pages: 55

Number of tables: 2

Number of figures: 12

Number of references: 40

Number of words in Abstract: 240

Number of words in Introduction: 749

Number of words in Discussion: 1500

Abbreviations: ACh, acetylcholine; D_i, type II PAM insensitive desensitization; D_s, type II PAM sensitive desensitization; MLA, methyllycaconitine; N, number of channels in patch; nAChR, nicotinic acetylcholine receptor; PAM, positive allosteric modulator; P_{open}, probability of channel opening; TM2, second transmembrane domain.

Molecular Pharmacology Fast Forward. Published on September 1, 2011 as DOI: 10.1124/mol.111.074302
This article has not been copyedited and formatted. The final version may differ from this version.

Structure-based names: 4O H2MeOBA, 3-(4-hydroxy, 2-methoxybenzylidene)anabaseine; 5HI, 5-hydroxyindole; A-867744, 4-(5-(4-chlorophenyl)-2-methyl- 3-propionyl-1*H*-pyrrol-1-yl)benzenesulfonamide; BTMPS, bis-(2,2,6,6-tetramethyl-4-piperidinyl) sebacate; diMeOBA, 3-(2,4-dimethoxybenzylidene)anabaseine; diOHBA, 3-(2,4-dihydroxybenzylidene)anabaseine; TQS, 3a,4,5,9b-Tetrahydro-4-(1-naphthalenyl)-3*H*-cyclopentan[*c*]quinoline-8-sulfonamide; tropisetron, (1R,5S)-8-methyl-8-azabicyclo[3.2.1]octan-3-yl 1methyl-indole-3-carboxylate; lobeline, 2-[6- (2-hydroxy- 2-phenyl- ethyl)- 1-methyl- 2-piperidyl]- 1-phenyl- ethanone; PNU-120596, *N*-(5-Chloro-2,4-dimethoxyphenyl)-*N*'-(5-methyl-3-isoxazolyl)-urea; PNU-282987, *N*-(3*R*)-1-Azabicyclo[2.2.2]oct-3-yl-4-chlorobenzamide.

Molecular Pharmacology Fast Forward. Published on September 1, 2011 as DOI: 10.1124/mol.111.074302
This article has not been copyedited and formatted. The final version may differ from this version.

Abstract

Although α7 nicotinic acetylcholine receptors are considered potentially important therapeutic targets, the development of selective agonists has been stymied by the α7 receptor's intrinsically low probability of opening (P_{open}) and the concern that an agonist-based therapeutic approach will disrupt endogenous cholinergic function. Development of α7 positive allosteric modulators (PAMs) holds promise of avoiding both issues. PNU-120596 is one of the most effective α7 PAMs, with a mechanism, at least in part, associated with the destabilization of desensitized states. We studied the mechanism of PNU-120596 potentiation of α7 receptors expressed in *Xenopus* oocytes and outside-out patches from BOSC 23 cells. We identify two forms of α7 desensitization: one is destabilized by PNU-120596 (D_s), and the other is induced by strong episodes of activation and is stable in the presence of the PAM (D_i). Our characterization of prolonged bursts of single-channel currents that occur with PNU-120596 provide a remarkable contrast to the behavior of the channels in the absence of the PAM. Individual channels that avoid the D_i state show a 100,000-fold increase in P_{open} compared to receptors in the non-potentiated state. In the presence of PNU-120596, balance between D_s and D_i is dynamically regulated by both agonist and PAM binding, with maximal ion channel activity at intermediate levels of binding to both classes of sites. In the presence of high agonist concentrations, competitive antagonists may have the effect of shifting the balance in favor of D_s and increasing ion channel currents.

Molecular Pharmacology Fast Forward. Published on September 1, 2011 as DOI: 10.1124/mol.111.074302
This article has not been copyedited and formatted. The final version may differ from this version.

Introduction

In the absence of agonist, ligand-gated ion channels are primarily in a resting, nonconducting state. With channels that mediate synaptic transmission when the resting condition is perturbed by a sudden elevation in agonist concentration, ligand binding sites become saturated and the energy landscape for transitions among the various conformational states of the receptor initially favors channel opening, producing periods of synchronous channel activation. Although the equilibrium between activated and non-conducting desensitized states may initially favor activation, desensitization occurs during all phases of a response, and in the prolonged presence of high concentrations of agonist, the ligand-bound receptors accumulate in the states with the lowest free energy; typically these are nonconducting desensitized states. This general behavior can be ascribed to all nicotinic acetylcholine receptor (nAChR) subtypes, but with some important differences between heteromeric and homomeric (α7) nAChRs.

Heteromeric nAChR such those found at the neuromuscular junction and autonomic ganglia contain two agonist binding sites (Millar and Gotti, 2009). They may open with a single agonist bound, but such openings are usually brief (Colquhoun and Sakmann, 1985) unless the single binding sites remain bound to agonist for prolonged periods of time (Williams et al., 2011a). The binding of agonist to both sites of a heteromeric receptor has a cooperative effect, increasing the probability of opening (P_{open}) and also promoting the stability of a long-lived open state (Williams et al., 2011a). Homomeric α7 nAChR also activate with submaximal agonist occupancy (Williams et al., 2011a), and the sort of positive cooperativity seen with heteromeric receptors does not appear to occur amongst the five putative agonist binding sites (Palma et al., 1996). Rapid saturation of the agonist binding sites on α7 receptors may increase the synchronization of whatever activation occurs, but net P_{open} is not increased through cooperative mechanisms, since saturating concentrations of agonist promote a form of rapid desensitization unique to homomeric α7 nAChR (Papke et al., 2000). The unique

Molecular Pharmacology Fast Forward. Published on September 1, 2011 as DOI: 10.1124/mol.111.074302
This article has not been copyedited and formatted. The final version may differ from this version.

desensitization of α7 nAChR can be induced rapidly, but it is also readily reversible after the removal of agonist (Papke et al., 2000).

Heteromeric receptors also desensitize rapidly, even at relatively low concentrations of agonist. However, they achieve an equilibrium between activation and desensitization that makes it possible to record prolonged macroscopic responses over a wide range of agonist concentrations (Papke, 2009). The desensitization of heteromeric nAChR does not usually reverse rapidly since these receptors bind agonist with very high affinity in the desensitized state (Heidmann and Changeux, 1978). Modeling these differences, we identify several key features which distinguish the energy landscapes for the conformational transitions of α7 from heteromeric nAChR including: higher energy barriers for entering the open state, low open state stability, a unique desensitized state, and relatively small energy differences between the resting and desensitized states.

While the intrinsically low P_{open} of α7 nAChR has presented a special challenge to the study of α7 activation at the level of single-channel currents, new tools have been developed in the form of positive allosteric modulators (PAMs) (Williams et al., 2011b). A number of chemically diverse PAMs have been identified and broadly classified into two groups based on their functional modulation of α7-mediated responses. The PAMs classified as type I, such as 5-hydroxyindole (5HI), reduce the height of energy barriers for transitions into active states, creating a transient increase in P_{open} immediately after agonist applications, but without altering the absolute energy differences between the states, resulting in potentiated responses with conserved kinetics. In contrast, type II PAMs, such as *N*-(5-Chloro-2,4-dimethoxyphenyl)-*N*'-(5-methyl-3-isoxazolyl)-urea (PNU-120596), not only increase the magnitude of responses immediately after agonist applications, but also alter the equilibrium between active and desensitized states resulting in dramatically prolonged responses, even promoting activation of previously desensitized receptors (Gronlien et al., 2007).

Molecular Pharmacology Fast Forward. Published on September 1, 2011 as DOI: 10.1124/mol.111.074302
This article has not been copyedited and formatted. The final version may differ from this version.

We have investigated the activation and desensitization of α7 nAChR at the level of macroscopic and single-channel currents, in the presence and absence of PNU-120596. We identify two forms of α7 desensitization. One is sensitive to and destabilized by PNU-120596 (D_s), and the other is insensitive (D_i) to the PAM and, in fact, promoted by high levels of PNU-120596 binding and potentiated activation. We hypothesize that D_s is associated with the rapid form of desensitization unique to α7, and in the presence of type II modulators, D_s is connected to an open state homologous to the long-lived open state observed in diliganded heteromeric nAChRs. We determine that, even in the presence of PNU-120596, optimal P_{open} may occur at levels of sub-maximal occupancy of the agonist and PAM binding sites, conditions which minimize stabilization of D_i.

Molecular Pharmacology Fast Forward. Published on September 1, 2011 as DOI: 10.1124/mol.111.074302
This article has not been copyedited and formatted. The final version may differ from this version.

Methods and Materials

cDNA clones used for heterologous expression in Xenopus oocytes and BOSC 23 cells

Human nAChR receptor clones and concatamers were obtained from Dr. Jon Lindstrom (University of Pennsylvania, Philadelphia PA). The human RIC-3 clone was obtained from Dr. Millet Treinin (Hebrew University, Jerusalem Israel) and co-expressed with α7 to improve the levels and speed of receptor expression (Halevi et al., 2002). The red fluorescent protein clone, pDsRed-N1, was obtained from Clontech (Palo Alto, CA) and used to identify successfully transfected BOSC 23 cells. The human α7 T6'S mutant was previously described (Placzek et al., 2005). The L9'T mutation, first characterized in chicken α7 (Bertrand et al., 1997) was inserted into the human cDNA using standard site-directed mutagenesis procedures with a QuikChange kit from Stratagene (La Jolla, CA) according to the manufacturer's instructions. The mutation was confirmed with automated fluorescent sequencing.

Heterologous expression of nAChR in Xenopus oocytes

Oocyte preparation: Oocytes were surgically removed from mature *Xenopus laevis* frogs and injected with 50 nl (5-20 ng) of appropriate nAChR subunit *in vitro* transcribed RNAs as described previously (Papke and Stokes, 2010).

Oocyte recording and data analysis

Experiments were conducted using OpusXpress 6000A (Molecular Devices, Union City California) and analyzed as previously described in detail (Papke and Stokes, 2010) using pClamp10 (Molecular Devices, Union City, CA) and Excel software (Microsoft, Redmond, WA). For all experiments evaluating the effects of PAMs, baseline conditions were defined by two control applications of 60 μM acetylcholine (ACh) made prior to the experimental applications. Test compounds were either applied into the bath using the

Molecular Pharmacology Fast Forward. Published on September 1, 2011 as DOI: 10.1124/mol.111.074302
This article has not been copyedited and formatted. The final version may differ from this version.

OpusXpress system for changing the running buffer or with the normal OpusXpress pipette delivery system. Data were subsequently normalized by calculating responses relative to the average peak current and net charge of the two initial control responses. A period of 120 s was used for the calculation of net charge in all experiments beginning at the start of the solution application.

Chemicals and synthesis of PNU-120596: Solvents and reagents were purchased from Sigma-Aldrich Chemical Company (St. Louis, MO), Fisher scientific (Pittsburg, PA) and TCI America (Portland, OR). PNU-120596 was synthesized following the method previously described (Piotrowski et al., 2003) for similar couplings. Specifically, reaction of 5-chloro-2,4-dimethoxyphenyl isocyanate (2.5 mmol) with one equivalent of 3-amino-5-methyl isoxazole in 50 mL dry benzene was maintained at 65 °C for 4 days. The reaction mixture was cooled down and concentrated to a solid in vacuo. The crude product was recrystallized three times from isopropanol, decolorized with activated carbon in isopropanol, and then filtered though a celite pad. After concentration, a fluffy white solid was obtained in 39% yield, having a melting point (219.5°C-220.5°C) identical to a commercially available sample from Tocris (St. Louis, MO). The purity and composition of PNU-120596 was further confirmed with NMR spectroscopy. ^{1}H NMR (300 MHz, acetone-d_6) δ 2.38 (d, J=0.88 Hz, 3 H) 3.89 (s, 3 H) 3.96 (s, 3 H) 6.41 (br. s., 1 H) 6.87 (s, 1 H) 8.31 (s, 1 H) 8.85 (br. s., 1 H) 9.13 (s, 1 H). The mass spectrum was obtained on an Agilent 6210 TOF spectrometer operated in ESI mode: m/z 334.0551 [M+Na]+ (calculated: 334.0565).

Cell culture and transient transfection of BOSC 23 cells

BOSC 23 cells obtained from American Type Culture Collection (Manassas, VA) were cultured at 37°C, 5% CO_2 in DMEM (Invitrogen, Carlsbad, CA) supplemented with 10% fetal bovine serum in the absence of antibiotics. Cells were discarded and fresh

Molecular Pharmacology Fast Forward. Published on September 1, 2011 as DOI: 10.1124/mol.111.074302
This article has not been copyedited and formatted. The final version may differ from this version.

cells thawed once 25 passages were reached. One day prior to transfection, cells were plated onto 12 mm glass coverslips (Fisher Scientific, Pittsburgh, PA) previously coated with Poly-D-Lysine (Sigma, St. Louis, MO). Cells were transiently transfected using Fugene 6 (Roche, Indianapolis, IN) according to the manufacturer's instructions. One μg, 0.3 μg, and 0.8 μg of plasmids containing cDNA clones of human α7, human RIC-3, and DsRed, respectively, with 6.3 μl of Fugene 6 reagent were added to each 35 mm dish containing cells and coverslips. Experiments were performed 48 to 72 hours after transfection.

Outside-out patch clamp electrophysiology

Single-channel currents were recorded in the outside-out patch configuration using an Axopatch 200A amplifier (Molecular Devices, Union City, CA) at room temperature. Cells were bathed in an external solution containing (in mM): NaCl (165), KCl (5), $CaCl_2$ (2), glucose (10), HEPES (5), atropine (0.001), pH adjusted to 7.3 with NaOH. Patch pipettes (Sutter Instruments, Novato, CA) were pulled to a tip diameter of 1-2 μm, fire-polished to 5–10 MΩ, coated with SigmaCote (Sigma, St. Louis, MO), and filled with an internal solution containing (in mM): CsCl (147), $MgCl_2$ (2), $CaCl_2$ (1), EGTA (10), HEPES (10), Mg-ATP (2), pH adjusted to 7.3 with CsOH. Recordings were low-pass filtered to 10 kHz with the built-in amplifier filter (4-pole Bessel) and digitized at 100 kHz with a DigiData 1440 (Molecular Devices, Union City, CA) using Clampex 10 data acquisition software (Molecular Devices, Union City, CA).

Rapid drug application to outside-out patches was performed with a Burleigh piezoelectric stepper (EXFO, Ontario, Canada) as described previously (Williams et al., 2011a). Theta glass (Sutter Instruments, Novato, CA) was pulled, scored, and then broken by hand to create a drug application pipette with a diameter of 120 μM (septum thickness: ~ 10 μM), which was mounted to the stepper. The voltage signal used to

Molecular Pharmacology Fast Forward. Published on September 1, 2011 as DOI: 10.1124/mol.111.074302
This article has not been copyedited and formatted. The final version may differ from this version.

control the piezoelectric stepper was conditioned by an RC circuit (τ = 2 ms) to reduce oscillations and avoid damage to the crystal.

Two solution reservoirs (60 ml Monoject syringes; Sherwood Medical, St. Louis, MO) were connected to each channel of the theta glass application pipette via polyethylene tubing; the tubing and application pipette could be completely primed with solutions from either reservoir within 15 s. Flow rates from each reservoir and channel of the drug application pipette were ~ 11 cm/s. Solution exchange times were typically between 0.4-0.7 ms (10%-90% rise-times) and were routinely determined by movement of diluted external solution over an open recording pipette. To maintain undisturbed laminar flow from the application pipette and minimize solution mixing, external saline solution was continuously perfused through the recording chamber (Warner Instruments, Hamden, CT) at a rate of 4 ml/minute, and the application pipette was positioned such that streams flowing from it would directly enter the aspiration port of the chamber. In addition, the tip of the application pipette was kept free of dirt and/or cell debris by periodic cleaning in a hydrochloric acid solution.

Patch-clamp recordings were analyzed with Clampfit 10 (Molecular Devices, Union City, CA) and QuB (University at Buffalo, Buffalo, NY) software. Sections of data traces with minimal simultaneous openings and flanked by ≥ 100 ms of closed time were selected for analysis. Following initial periods of multi-channel openings, single-channel bursts potentiated by PNU-120596 occurred in very obvious groups of openings that were separated by long silent periods. This characteristic eliminated the ambiguity that is normally associated with defining a burst delimiter value (t_{crit}) used in burst analysis of single-channel recordings (Colquhoun and Sakmann, 1995). The t_{crit} value used to determine average burst duration intervals was 150 ms; large variations in this value had minimal impact on the outcome of burst analysis. To determine intraburst closure, subconductance, and open durations, a total of 40 protracted bursts were selected at random for careful idealization. Data traces were idealized within QuB using the

Molecular Pharmacology Fast Forward. Published on September 1, 2011 as DOI: 10.1124/mol.111.074302
This article has not been copyedited and formatted. The final version may differ from this version.

segmental k-means method (Qin, 2004) and were idealized at a bandwidth of 10 kHz, but the sampling rate was reduced from 100 kHz to 30 kHz to improve the quality of idealization since segmental k-mean idealization is generally optimized at or near the Nyquist frequency (F. Sachs, personal communication via QuB user forum). Following the automated idealization, the fit was manually inspected event-by-event and corrections were made as necessary to the idealization. A temporal resolution limit of 1.3 x filter rise-time was set at 40 μsec and imposed in all analyses. The probability of channel opening was determined by the equation,

$$NP_{open} = \frac{1}{iD}\int_0^D I(t)dt$$

where I is the recorded current relative to baseline, t is time, i is the mean single-channel amplitude, D is the duration of the drug application, and N is the number of channels in the patch. Of course, N is always unknown and the P_{open} measurement is only as accurate as the estimate of N.

Molecular Pharmacology Fast Forward. Published on September 1, 2011 as DOI: 10.1124/mol.111.074302
This article has not been copyedited and formatted. The final version may differ from this version.

Results

ACh-evoked responses of α7 nAChR expressed in Xenopus oocytes.

The agonist-evoked responses of α7 nAChR have unique features which distinguish them from the responses of other nAChR subtypes and are important to consider to provide a context for how an allosteric modulator may work to increase those responses. Typically, the ACh-evoked responses of heteromeric nAChR increase during the application of agonist at a rate consistent with the speed of solution exchange and subsequently decay after solution exchange is complete, as illustrated in Figure 1A. In our oocyte recording system the time constant for solution exchange is 3-4 seconds, matching the rise and decay of α4β2-mediated currents, in this case associated with the low sensitivity form of the receptor containing three α4 and two β2 subunits (Zhou et al., 2003). It should be noted that the apparent plateau of the α4β2-mediated currents during the agonist application does not indicate that these receptors do not desensitize, but rather that the processes of activation and desensitization are both more rapid than the solution exchange and are therefore more or less at equilibrium during the plateau phase of the response (Papke, 2009). Due to the stability of these equilibrated responses during the agonist applications, the concentration-response relations for peak currents and net charge are essentially identical.

In contrast to responses of heteromeric nAChR, the responses of α7 nAChR evoked by the application of high concentrations of agonist (Figure 1B) reach a peak before solution exchange is complete (Papke and Thinschmidt, 1998), so that large peak currents are indicative of synchronized activation but not increased receptor activation over the duration of the agonist application. This is reflected in the disparity between the apparent concentration-response relationships for α7 peak currents and net charge. It is therefore fundamentally a fallacy to attribute large peak current responses to high concentrations of agonist, and by inference high levels of agonist binding site occupancy,

Molecular Pharmacology Fast Forward. Published on September 1, 2011 as DOI: 10.1124/mol.111.074302
This article has not been copyedited and formatted. The final version may differ from this version.

since little or no current is recorded under the conditions when agonist concentration is very high.

Activation of α7 nAChR occurs when there is only fractional occupancy of the agonist binding sites (Williams et al., 2011a), and the decreased P_{open} at higher levels of agonist occupancy is consistent with a form of agonist concentration-dependent desensitization unique to α7. One of the effects of the type II α7 PAM PNU-120596 is to reverse or destabilize one or more forms of α7 receptor desensitization. As shown in Figure 1C, the ACh-evoked responses of α7 nAChR recorded in the presence of PNU-120596 lacked the appearance of concentration-dependent desensitization. Consistent with the reversal of a form of desensitization that is unique to α7, in the presence of PNU-120596, the ACh concentration-response relationships for peak current and net charge were essentially identical, as is the case with heteromeric nAChR.

ACh-evoked responses of α7 nAChR expressed in BOSC 23 cells in absence and presence of PNU-120596.

A typical response of an outside-out patch expressing α7 to rapid application (≤0.7 ms) of 60 μM ACh is shown in Figure 2A. Channel openings occur with highest frequency immediately after application of ACh and then quickly disappear despite continued application of agonist. Individual α7 channel openings are extraordinarily brief, and appear primarily as isolated events rather than bursts of openings. At a bandwidth of 10 kHz, the average duration of the apparent α7 single-channel openings evoked by 60 μM ACh is 113 ± 7 μs (n = 187 openings, 13 patches). Considering that this short duration lies just above temporal resolution limits, many openings probably occurred that were too short to be reliably detected, and the average α7 open duration is over-estimated. Figure 2B displays a histogram of the apparent channel openings fit by a single exponential function. Assuming the distribution of the missed openings follows the fit exponential function to the ordinate, the corrected average α7 single-channel open

Molecular Pharmacology Fast Forward. Published on September 1, 2011 as DOI: 10.1124/mol.111.074302
This article has not been copyedited and formatted. The final version may differ from this version.

duration is 59 ± 5 μs. At a holding potential of -70 mV, the average single-channel amplitude of the apparent α7 openings was -6.22 ± 0.08 pA. Given that individual α7 openings were so short in duration, this value may be an under-estimate of the true single-channel amplitude. A scatterplot of channel amplitude versus open duration showed no clear overall relationship. However, all openings longer than 300 μs in duration had single-channel amplitudes between -6.8 pA and -7.6 pA (not shown).

The type II PAM PNU-120596 had a profound impact on responses evoked by 60 μM ACh from outside-out patches (Figure 2C). In the absence of PNU-120596, responses evoked by 12 second applications of 60 μM ACh were limited due to the low P_{open} intrinsic to α7 and may lead one to believe the patch contains few channels. A follow-up application of 60 μM ACh with 10 μM PNU-120596 to the same patch revealed that in reality the patch contained a multitude of channels, demonstrating the massive potential for enhancement of α7 responses by PNU-120596. The net charge response evoked by co-application of 60 μM ACh and 10 μM PNU-120596 was on average $1.35 \times 10^{-5} \pm 0.42 \times 10^{5}$-fold larger than the net charge response evoked by 60 μM ACh alone (n = 4).

The peak current of the response evoked by ACh and PNU-120596 co-application, divided by the unitary current amplitude of PNU-120596-potentiated currents, provides a lower-limit estimate of the number of channels in a patch (N). The number of channels in each patch is an unknown, but is a parameter of interest since it is required to calculate P_{open}. The ACh and PNU-120596 concentration combination that evokes maximal peak responses is important to know in order to obtain a lower-limit estimate of N that is as accurate as possible. We performed several experiments with *Xenopus* oocytes expressing α7 testing various concentration combinations of ACh and PNU-120596 and found that a range of ACh (10 – 100 μM) concentrations with 10 μM PNU-120596 provided comparable maximal peak currents (data not shown). We calculated, based on the detected α7 openings in the absence of PNU-120596 and the

Molecular Pharmacology Fast Forward. Published on September 1, 2011 as DOI: 10.1124/mol.111.074302
This article has not been copyedited and formatted. The final version may differ from this version.

lower-limit of N provided by peak currents in response to 60 μM ACh and 10 μM PNU-120596 co-application, an upper-limit estimate of α7 P_{open} in response to a 1 2 second application of 60 μM ACh of 7.4 x 10^{-6} ± 3.0 x 10^{-6} (n = 4). It is important to understand that this estimate is strictly an upper-limit estimate since N is unknown and potentially greatly underestimated. A lso, it is equally important to appreciate that this estimate includes the non-stationary portion of the 60 μM ACh-evoked responses, immediately after application of ACh when channel activation occurs with highest probability, and that under true steady-state conditions the upper-limit α7 P_{open} will be much less.

The potentiation of α7-mediated currents in Xenopus oocytes by PNU-120596 does not reflect the functional conversion of previously inactive receptors.

Aside from the unitary conductance and driving force, which we may assume are constants in all voltage clamp experiments, macroscopic current responses such as those recorded in the *Xenopus* oocyte expression system depend on t wo factors that will vary from cell to cell and experiment to experiment: the total number of activatible receptors and the P_{open} of each single receptor. Hypothetically, a PAM may operate on any of these factors to increase the magnitude of agonist-evoked responses. Since it has been reported that in some neuronal cell systems the majority of surface α7 receptors (McNerney et al., 2000) are not in fact readily activatible, we wished to determine if PNU-120596 operated on the same population of rec eptors that were activatible in the absence of th e PAM, or alternatively, increase the number of receptors available for activation. To test this we, co-applied ACh with the slowly reversible use-dependent inhibitor bis-(2,2,6,6-tetramethyl-4-piperidinyl) sebacate (BTMPS; (Papke, 1993)) and measured the recovery of ACh-evoked responses eight minutes later (Figure 3A). At that time, there was still approximately 60% inhibition relative to the initial ACh-evoked responses. We t hen measured the responses stimulated by co-applications of 60 μM ACh and 10 μM PNU-120596 with or without prior BTMPS-induced inhibition. Responses were normalized to

Molecular Pharmacology Fast Forward. Published on September 1, 2011 as DOI: 10.1124/mol.111.074302
This article has not been copyedited and formatted. The final version may differ from this version.

initial ACh controls, and we determined that the relative inhibition of the PNU-120596-potentiated responses was not different from the relative inhibition of the non-potentiated responses (Figure 3B), indicating that it is unlikely that PNU-120596 potentiation involves increasing the number of activatible receptors.

Convergence and competition of type I and type II PAM activity and PAM effects on "gain-of-function" mutants.

Studies of chimeric receptors and receptors with site-directed mutations have implicated points of contact between extracellular and transmembrane domains as being important for mediating the potentiating effects of both type I and type II PAMs, while it has been proposed that the actual binding site for PNU-120596 is in a water-filled space amongst the transmembrane alpha helices (Young et al., 2008). As shown in Figure 4A, co-application of the prototypical type I PAM 5HI with PNU-120596 significantly reduced potentiation compared to the effects of PNU-120596 alone ($p < 0.05$). Such competition between type I and type II PAMs might occur at either of two levels: through competition at a common binding site or through mechanistic interference at sites required to obtain the effects of either class of compound.

Multiple types of α7 "gain-of-function" mutations have been reported, most of which are associated with sequence changes in the second transmembrane domain (TM2), which is believed to line the ion channel. To varying degrees, the effects of these mutations mimic some of the effects of PAMs. We wished to determine the degree to which PAM activity relied on wild-type sequence at these sites and whether the activity of both type I and type II PAMs were perturbed in the same manner and to the same degree by specific mutations. The substitution of a serine for threonine at the sixth residue in the α7 TM2 (T6'S; (Placzek et al., 2005)) produces a modest gain of function with features resembling those produced by a type I PAM. The peak macroscopic currents of α7T6'S mutants are large compared to wild-type α7, and single-channel open

Molecular Pharmacology Fast Forward. Published on September 1, 2011 as DOI: 10.1124/mol.111.074302
This article has not been copyedited and formatted. The final version may differ from this version.

times are prolonged, sometimes occurring in short bursts (Placzek et al., 2005). However, as is the case with wild-type receptors modified by a type I PAM, the currents of α7T6'S mutants decay to baseline during the application of a high concentration of agonist (Figure 4B). These effects of the T6'S mutation are relatively subtle compared to the well-studied mutation at the 9' position in TM2, L9'T (Bertrand et al., 1997). The effects of this mutation are so extensive that arguably it might be called a "perversion-of-function" as much as a "gain-of-function" since, unlike the T6'S mutants which preserve the pharmacological distinction between agonists and antagonists, α7L9'T mutants may be activated by agents which are antagonists of wild-type receptors. The α7L9'T mutants generate currents that are very large (Figure 4B), and it has been proposed that the mutation destabilizes a desensitized state or converts it into a conducting conformation, an effect which has also been proposed for the potentiation of wild-type α7 by PNU-120596.

As shown in Figure 4C, the effects of the type I PAM 5HI on α7T6'S receptors were similar to the effects on wild-type α7, although proportionately somewhat smaller due to higher initial control responses. In contrast, 5HI behaved more like an agonist than a PAM on α7L9'T receptors since activation occurred in response to the pre-application of 5HI alone and was not much increased when ACh was co-applied. In fact, the responses of the α7L9'T receptors to ACh in the presence of 5HI were less than responses to ACh alone. Likewise, the effects of PNU-120596 on α7T6'S receptors were similar to the effects on wild-type α7, albeit somewhat smaller when compared to initial controls, while the α7L9'T mutants showed a response to the application of the PAM in the absence of agonist, and smaller responses to ACh plus PNU-120596 than to ACh alone (Figure 4D).

These data suggest that the effects of the T6'S mutation are not additive, synergistic, or antagonistic to the effects of the PAMs tested, while the α7L9'T mutant is a poor model for the mechanism of PNU-120596 potentiation. Although both PNU-

Molecular Pharmacology Fast Forward. Published on September 1, 2011 as DOI: 10.1124/mol.111.074302
This article has not been copyedited and formatted. The final version may differ from this version.

120596 and the mutation appear to disrupt a form of desensitization that is unique to α7, the effects of PNU-120596 still have a strict requirement for some agonist binding.

Factors limiting the potentiating effects of PNU-120596 on α7-mediated currents.

We investigated the time and concentration dependence of PNU-120596 potentiation of wild-type human α7 nAChR responses by making repeated applications of 60 μM ACh in the presence of varying bath concentrations of PNU-120596 over the course of one hour. Maximal potentiation of peak current amplitude was achieved with 10 μM PNU-120596, although the maximal potentiation of net charge was similar in the presence of both 10 and 30 μM (Figure 5A). Interesting concentration-dependent effects were seen on the onset and decline of potentiation (Figure 5B). In the presence of 0.3 μM PNU-120596 potentiation increased throughout the experiment, with potentiation significantly ($p < 0.01$) larger at 64 minutes than at 12 minutes. In the presence of 1 μM PNU-120596, potentiation was greater at 40 minutes than at 12 minutes ($p < 0.05$), but not significantly greater at 64 minutes than at 12 minutes. For all concentrations of PNU-120596 ≥ 3 μM, the potentiation reached a maximum level within approximately 10-20 minutes and then decayed, with potentiation significantly less at 64 minutes than that at 12 minutes ($p < 0.05$). These data support the hypothesis that, although some of the mechanism of PNU-120596 may involve the relief or reversal of a sensitive form of desensitization (D_s), strong or protracted stimulation in the presence of PNU-120596 promotes the conversion of the receptor into an alternative PNU-120596-insensitive desensitized state (D_i).

To evaluate the ACh concentration dependence of responses potentiated by PNU-120596, 1 μM and 100 μM ACh were applied to an outside-out patch expressing α7 with the PNU-120596 concentration fixed at 10 μM (Figure 6). Neither the peak current nor the net charge were different in these experiments between responses evoked by 1 μM ACh or 100 μM ACh in the presence of 10 μM PNU-120596. However, the onset and

Molecular Pharmacology Fast Forward. Published on September 1, 2011 as DOI: 10.1124/mol.111.074302
This article has not been copyedited and formatted. The final version may differ from this version.

decay of the potentiation were different. Responses evoked by 1 μM ACh in the presence of 10 μM PNU-120596 had significantly ($p < 0.05$) slower 10%-90% rise-times than responses evoked by 100 μM ACh and 10 μM PNU-120596 (12.3 ± 5.1 s versus 1.4 ± 0.5 s; n = 4). Responses evoked by 100 μM ACh tended to peak relatively rapidly and then decay despite the continued application of ACh and PNU-120596, while responses evoked by 1 μM ACh generally showed little-to-no decay on the time scale of these recordings. The ratio of the net charge during the last quarter of the response relative to the first quarter of the response was 1.35 ± 0.28 with 1 μM ACh, whereas the ratio was 0.39 ± 0.08 in the 100 μM ACh condition. The average 90%-10% decay time of 100 μM ACh and 10 μM PNU-120596 responses was 26.14 ± 3.52 s (n = 4).

In order to test the hypothesis that the induction of D_i is dependent on receptor activation, we treated oocytes with one of two different stimulus protocols (Figure 7A). In the continued presence of 3 μM PNU-120596, oocytes were either repeatedly stimulated with 10 μM ACh or with 10 μM ACh applications in alternation with stronger stimulation by 300 μM ACh. As shown in Figure 7B, the 10 μM ACh-evoked responses of cells stimulated alternately with 300 μM ACh reached a level of maximal potentiation relatively quickly and then showed a decline, consistent with the induction of D_i. In contrast, the 10 μM ACh-evoked responses of oocytes that did not receive alternating application of 300 μM ACh were slower to reach the same level of maximal potentiation, but also no decline in potentiation occurred over the course of an hour. Together these results suggest that both agonist and PNU-120596 concentrations affect the time course of potentiated responses, with faster onset of potentiation and subsequent decay occurring at high concentrations, and low concentrations producing relatively slow rising, but longer-lasting currents.

Although α7 nAChRs desensitize rapidly in response to high concentrations of agonist, the desensitization is also rapidly reversible once agonist has dissociated from the receptor (Papke et al., 2000). We tested whether the PNU-120596-insensitive form of

Molecular Pharmacology Fast Forward. Published on September 1, 2011 as DOI: 10.1124/mol.111.074302
This article has not been copyedited and formatted. The final version may differ from this version.

desensitization that developed with strong stimulation in the presence of the PAM was also readily reversible. As shown in Figure 8A, if repeated co-applications of 60 μM ACh and 10 μM PNU-120596 to oocytes were stopped during the period of time when insensitive desensitization was developing and later reinitiated, the receptors became resensitized to the effects of the PAM. Likewise, recovery from D_i induced by 300 μM ACh and 10 μM PNU-120596 occurred in outside-out patches in experiments performed with a much shorter timescale (Figure 8B).

Single-channel bursts of α7 nAChR promoted by PNU-120596

Because the potentiation of responses by PNU-120596 is so profound, we initially reasoned that the probability of observing single-channel currents potentiated by PNU-120596 would be low. However, the decay of current was so pronounced with prolonged long applications of 300 μM ACh and 10 μM PNU-120596 that single-channel bursts potentiated by PNU-120596 were revealed once the majority of channels entered the D_i state(s) (Figure 9A). From three patches with sections of continuous data > 60 seconds lacking simultaneous channel openings, the steady-state absolute P_{open} (NP_{open}) in 300 μM ACh and 10 μM PNU-120596 was 0.40 ± 0.04. Given the length of the single-channel bursts and the lack of simultaneous openings in these traces, it seems that the number of activatible channels at any time is greatly limited by D_i. It is unknown whether the openings in these traces all arise from one resilient channel that escaped and remained resistant to D_i, or whether the openings arose from multiple channels as they temporarily escaped D_i.

There appeared to be two qualitatively distinct groups of single-channel openings in the presence of PNU-120596 (Figure 9A). One class of PNU-120596-potentiated opening appeared as relatively brief events that primarily occurred in isolation, and the other, more common, type of PNU-120596-potentiated openings appeared to occur as long bursts of openings separated by very short closures to either fully closed or

Molecular Pharmacology Fast Forward. Published on September 1, 2011 as DOI: 10.1124/mol.111.074302
This article has not been copyedited and formatted. The final version may differ from this version.

subconductance states. Most of the brief type of openings observed in the presence of PNU-120596 were < 1 ms in duration, occasionally lasting approximately 8 ms (Table 1). A major component of the isolated openings evoked in the presence of PNU-120596 was fit with a time constant of 120 ± 6 μs, which is similar to the average apparent open duration in the absence of PNU-120596.

On average, the long bursts of openings potentiated by 10 μM PNU-120596 persisted for 5.48 ± 0.40 s (n = 217, 26 patches). The majority of the apparent intraburst closures were approximately 100-200 μs; however, occasionally intraburst closures longer than approximately 10 ms were observed. The subconductance events were approximately 400 μs or less in duration and were interrupted by many fast full channel closures (Figure 9A inset, Table 1). There appeared to be two distinct classes of the long PNU-120596-potentiated bursts; the distinction was made based on the duration of the intraburst openings (Figure 9B, Table 1). Approximately 27% of the bursts analyzed exclusively contained intraburst openings of approximately 5 ms in duration (class I bursts) and 73% of the bursts exclusively contained intraburst openings of approximately 30 ms in duration (class II bursts). No clear relationship was apparent between burst length and average intraburst open durations (Figure 9B) and the apparent closed and subconductance duration intervals were similar between the two classes of bursts (Table 1). The reason for the two types of bursts is unclear, but may be related to occupancy of ACh and/or PNU-120596 at their respective binding sites during the burst of openings.

At a holding potential of -70 mV, the single-channel amplitude of openings potentiated by PNU-120596 was -7.76 ± 0.08 pA, and the subconductance level amplitude was -3.59 ± 0.02 pA. The current-voltage relationship of currents evoked in the presence of PNU-120596 showed strong inward rectification, a reversal potential of -6.93 ± 1.01 mV, and a single-channel chord conductance of 129 ± 3 pS through the linear section of the relationship (n = 6, data not shown). Given that PNU-120596 appears to have little, if any, effect on channel conductance (Hurst et al., 2005), the conductance

Molecular Pharmacology Fast Forward. Published on September 1, 2011 as DOI: 10.1124/mol.111.074302
This article has not been copyedited and formatted. The final version may differ from this version.

measured in the presence of PNU-120596 is likely to be a reasonable estimate of single-channel α7 conductance in the absence of PNU-120596. This measurement is higher than the previously published values of 60-90 pS (McNerney et al., 2000; Mike et al., 2000), but the difference is probably related to the limited ability to accurately measure α7 open channel amplitude in the absence of PAM, since non-potentiated α7 openings are so brief.

A phenomenon observed with currents from the outside-out patches that had been activated with ACh and potentiated by PNU-120596 was a postponed return to baseline after the removal of external ACh (Figure 9C). For single-channel bursts activated in the presence of 300 μM ACh and 10 μM PNU-120596, currents persisted for 2.57 ± 0.2 s following the removal of external ACh (n = 143, 15 patches). There was no detectable change of intraburst open durations, nor was there an apparent trend toward change in intraburst open duration over time after ACh removal. The protracted currents were not an artifact of slow or incomplete solution exchange, based on three arguments. First, following data collection each patch was blown off the tip of the pipette and solution exchange profiles were determined by measuring changes in holding current upon moving diluted saline over the open pipette tip with the piezoelectric stepper (Figure 9D). Data were analyzed only if the solution exchange profile measured in this way was clean and occurred rapidly, within ~700 μs (10%-90% rise-time). Typical solution exchange times measured with this method were between 400 μs and 700 μs. Second, there was a sharp reduction in current noise that was intimately associated with the removal of external ACh (Figure 9D). This reduction in noise was likely due to relief of channel block by ACh, given that a relatively high concentration was used as the stimulating agonist (Colquhoun and Sakmann, 1985). This reduction in current noise was highly significant ($p < 3 \times 10^{-15}$), as measured by changes in the standard deviation from the mean open current before and after removal of external ACh ($\sigma = 0.44 \pm 0.008$ versus 0.31 ± 0.003). Third, replacement of external ACh with the competitive α7 antagonist

Molecular Pharmacology Fast Forward. Published on September 1, 2011 as DOI: 10.1124/mol.111.074302
This article has not been copyedited and formatted. The final version may differ from this version.

methyllycaconitine (MLA) greatly attenuated the duration of the protracted currents (see below). The currents that persisted long after the removal of external ACh are consistent with the prolonged retention of ACh at the binding sites when PNU-120596 is applied. However, this observation could also be explained by maintenance of the channel in a reverberating conducting condition by PNU-120596 after dissociation of ACh on termination of external ACh application.

We attempted to test the hypothesis that PNU-120596 prolongs the retention of ACh to its binding site by removing external ACh and replacing it with 3 μM MLA. We initially reasoned that if the affinity of the agonist binding site for ACh was increased by PNU-120596, application of the high MLA concentration would have little effect on the duration of protracted currents, given that the channel was both occupied by ACh and in an activated condition on application of MLA. When ACh was replaced with MLA, the currents persisted for 0.22 ± 0.03 s (n = 25, 3 patches) after removal of external ACh, a significant ($p < 1 \times 10^{-5}$) reduction of the protracted current duration (Figure 9E).

Interestingly, the effect of MLA, which is normally considered a competitive antagonist, had the appearance of an inverse agonist in these experiments, given that channels were active when MLA was applied, and MLA shortened burst activity under conditions when no external ACh was available for competition. Prior to moving the patches out of the solution containing 300 μM ACh, we believe it is reasonable to assume that the five agonist binding sites of α7 were occupied by ACh at high probability. Further, we would hypothesize that after the removal of external ACh, agonist molecules began to dissociate one-by-one until the last ACh molecule dissociated, perhaps resulting in termination of the burst. When external ACh was removed and individual ACh molecules began to dissociate, MLA may have had the opportunity to bind the receptor in the vacant binding sites and terminate the burst before all ACh molecules had dissociated. Our data suggest that binding of only one or two molecules of MLA may be sufficient to inactivate the entire receptor and that MLA may actively inhibit channel gating, perhaps

Molecular Pharmacology Fast Forward. Published on September 1, 2011 as DOI: 10.1124/mol.111.074302
This article has not been copyedited and formatted. The final version may differ from this version.

by stabilizing non-conducting receptor conformations, rather than simply occupying the cavity where ACh binds to produce channel activation.

Multiple phases of PNU-120596-promoted currents during prolonged co-applications with agonists in Xenopus oocytes

Since PAMs are in therapeutic development, it is important to characterize their activity under conditions when they are present for long periods of time at relatively fixed concentrations. Likewise, we do not know the temporal character of the ACh and/or choline presentation to α7 nAChR in the brain, which may well involve oscillations on the time scale of seconds or longer. Therefore we investigated the time and concentration dependence of PNU-120596/agonist interactions on a protracted time scale to characterize both transient and potential steady-state effects.

Due to the induction of D_i as a function of the level of receptor activation, it was expected there would be variations in the time course and level of equilibrium potentiation, depending on the agonist and PNU-120596 concentrations. The multiple phases of α7 receptor activation produced by bath co-application of 3 μM PNU-120596 and varying concentrations of ACh are shown in Figure 10A (all traces are scaled relative to the amplitude of the initial ACh controls). There were two phases of potentiated current in all of these evoked responses: a fast transient peak and a subsequent slow phase. The peaks of the transient currents occurred faster with higher concentrations of ACh (Figure 10C). Although the timing of the transient peaks changed progressively through the range of ACh concentrations tested, the heights of the transient currents were greatest for the 30 μM ACh and 3 μM PNU-120596 co-applications (Figure 10D).

The slow phases of the potentiated responses were also dependent on ACh concentration. For example, the slow phase of the response evoked by 300 μM ACh and 3 μM PNU-120596 shown in Figure 10A reached a peak and began to decline by the end

Molecular Pharmacology Fast Forward. Published on September 1, 2011 as DOI: 10.1124/mol.111.074302
This article has not been copyedited and formatted. The final version may differ from this version.

of the 30 minute application, while the response evoked by 6 μM ACh and 3 μM PNU-120596 was still rising after 30 minutes.

After just 10 minutes of co-application, the steady-state currents measured in the experiments shown in Figure 10 were on average 6.5 ± 0.8 μA, representing approximately one million simultaneously open receptors. Although in each separate experiment at least 6 cells survived for the first 10 minutes, many cells could not be held in voltage-clamp for the entire 30 minute protocol with such high holding currents. Therefore we restricted the measurement of response features to the first 10 minutes of the responses in order to have 6-8 observations for each condition. Although the transient peaks of the 6 μM responses were lower than those of the 30 μM responses, the net charge accumulated during the transient phases of the 6 μM responses was a greater fraction of the total net charge in the first 10 minutes of the responses than that of any of the other conditions (Figure 10D, right hand Y axis, $P < 0.001$).

Clearly the slow and fast phases of the responses obtained by ACh co-applications with 3 μM PNU-120596 were differentially affected by ACh concentrations. The data presented in Figure 5 suggest that the concentration of PNU-120596 will also be a factor, such that sustained currents may be less readily obtained with higher concentrations of the PAM. Figure 10B shows comparisons between the responses evoked by 30 or 300 μM ACh co-applied with either 3 or 10 μM PNU-120596. The peaks in the transient phase of the responses occurred more rapidly in the presence of the higher concentration of PNU-120596 (Figure 10E, $p < 0.05$), and the total net charge in the first ten minutes of the responses was less with the higher concentration of the PAM (Figure 10F, $p < 0.001$), suggesting fast induction and greater levels of PAM-insensitive desensitization with the higher concentration of PNU-120596.

Molecular Pharmacology Fast Forward. Published on September 1, 2011 as DOI: 10.1124/mol.111.074302
This article has not been copyedited and formatted. The final version may differ from this version.

Varying concentration-dependent effects of competitive antagonists modulate P_{open} of PNU-120596-primed receptors.

Our data suggest that optimal steady-state activation of α7 nAChR by combinations of agonists and PNU-120596 will be achieved when there is submaximal occupancy of both the agonist and PAM binding sites. To test this hypothesis, we made applications of varying concentrations of the α7-selective competitive antagonist MLA to receptors responding to bath application of 3 μM PNU-120596 and different concentrations of the α7-selective agonist choline. The applications of MLA would be expected to change the fractional occupancy of the agonist binding sites, and, indeed, the effects of the MLA applications were observed to vary as a function of the choline concentrations. At the highest concentration of choline (600 μM, responses roughly equivalent to 60 μM ACh (Papke and Papke, 2002)) applications of both 10 nM and 100 nM MLA were observed to actually produce transient increases in the current during the slow phase of the responses, and the 1 μM application produced a relatively small decrease in current (with a positive rebound). These effects are compared in Figure 11 to the effect of a subsequent application of 100 μM mecamylamine, a noncompetitive antagonist. These concentration-dependent effects of MLA shifted progressively when the choline concentrations were reduced. In the presence of 200 μM choline, only the 10 nM MLA applications had purely positive effects, 100 nM had a biphasic effect, and the inhibition produced by 1 μM MLA was more similar to that produced by 100 μM mecamylamine. Consistent with this pattern, in the presence of 60 μM choline, 10 nM MLA had biphasic effects, and higher concentrations were purely inhibitory, with 1 μM fully as effective as 100 μM mecamylamine. The effect of MLA applications were confirmed to rely on α7 receptor activation due to the combination of agonist and PNU-120596 since MLA application had no detectable effect on cells expressing α7 and perfused with 3 μM PNU-120596 alone (not shown). It was also confirmed that the

Molecular Pharmacology Fast Forward. Published on September 1, 2011 as DOI: 10.1124/mol.111.074302
This article has not been copyedited and formatted. The final version may differ from this version.

effects of different MLA concentrations were independent of the order in which they were applied (not shown).

MLA is a large molecule, possibly capable of interacting with α7 nAChR in multiple ways. In order to confirm that the effects illustrated in Figure 11A were through MLA's activity as a competitive antagonist, we tested the effect of dihydro-β-erythroidine (DHβE), a competitive antagonist with selectivity for α4-containing nAChR but also active on α7 with an IC_{50} of approximately 8 μM (Papke et al., 2008). As shown in Figure 11B, applications of the two lower concentrations of DHβE produced transient increases in the currents that were activated by 200 μM choline in combination with 3 μM PNU-120596, while the highest concentration of DHβE had a biphasic effect.

Note that in the oocyte system, the effects of priming the receptors with PNU-120596 applications are reversed relatively slowly (Papke et al., 2009), presumably due to delayed dissociation of the PAM from its binding sites. Therefore in the experiments illustrated in Figure 11, follow-up control applications of ACh were much larger than the initial ACh controls. The amplitudes of those responses were strongly influenced by the choline concentration in the preceding bath applications, further indicating that the higher choline concentrations promoted more PAM-insensitive desensitization.

Specific ligands differentially regulate the stability receptors in the D_s and D_i states.

Although full and partial agonists differ in their effectiveness for ion channel activation, when applied at high concentrations for long periods of time, both types of drugs desensitize α7 nAChR so that they are unable to be activated by a further application of a full agonist. Since our data indicate the there are at least two different α7 desensitized states that can be distinguished based on their sensitivity to PNU-120596, we determined whether specific ligands selectively promoted the stability of either the D_s or D_i forms of the receptor. Specifically, we compared ACh to three α7-selective benzylidene anabaseine partial agonists, the structurally unrelated α7-selective agonist

Molecular Pharmacology Fast Forward. Published on September 1, 2011 as DOI: 10.1124/mol.111.074302
This article has not been copyedited and formatted. The final version may differ from this version.

tropisetron, and the very weak α7 partial agonist lobeline (Table 2). We applied these compounds for 5 minutes at relatively high effective concentrations (Papke et al., 2009; Papke et al., 2005) to two sets of oocytes expressing human α7 nAChR. We recorded varying levels of transient current during the initial moments of the drug application (Table 2, evoked response), and in all cases these currents declined to baseline by the end of the 5 minute incubation. One set of cells was then given an additional 1 mM ACh application to determine if the receptors were fully desensitized. Responses to this follow-up application of ACh were only detected if the cells had been incubated with anabaseine or lobeline (Table 2, ACh residual); for all other treatments desensitization appeared to be complete. To determine the relative expression of D_s and D_i, the second set of cells received an application of 300 μM PNU-120596 in the drug-containing incubation solution. The PNU-120596-evoked responses varied greatly and were not correlated to the apparent efficacy of the compounds on initial application (Table 2, PAM-evoked). Of the compounds which were fully desensitizing at the end of the 5 minute incubations, ACh and tropisetron were most effective at placing the receptors in the D_s state, based on the subsequent responses to the drugs plus PNU-120596. The benzylidene anabaseine compounds, which were all of comparable efficacy in the initial phase of the incubation and equally desensitizing after 5 minutes, differed by over a factor of 10 in the induction of D_s. Structurally these molecules differ only in the disposition of hydroxyl or methoxy side groups on the benzylidene ring, a portion of the molecule associated with α7 selectivity, but located a considerable distance from the cationic core pharmacophore (Papke et al., 2009).

Energy landscape models provide a qualitative description of a7 activation and desensitization.

Basic models of nAChRs are required to account for closed states (C), open states (O), and desensitized states (D) and integrate the effects of agonist binding and the

Molecular Pharmacology Fast Forward. Published on September 1, 2011 as DOI: 10.1124/mol.111.074302
This article has not been copyedited and formatted. The final version may differ from this version.

relative occupancy of these states. The model in Figure 12 describes the receptor's functional states based on hypothetical relative free energy levels and intervening energy barriers through a matrix of increasing occupancies at both agonist and PAM binding sites. The relative energy levels and heights of the energy barriers are proportionate to the logs of the transition rate constants in standard Markov models. The model is minimal and omits potential intermediate states, such as the hypothetical flip state (Lape et al., 2008), but effectively represents qualitative characteristics of our data. Vertical distances represent absolute differences in free energy, or stability, and will be predictive of the relative occupancy of the various states under equilibrium conditions. To simplify comparisons between the schematics for the various levels of agonist occupancy, the resting closed states were set to the same level. However, it should be appreciated that the average free energy of the resting bound state for each schematic probably increases (becomes less stable) in a step-wise manner as agonist occupancy increases. Also, it should be noted that the hypothetical energy landscapes in Figure 12 are designed to explain our data for the full agonists ACh and choline, and the energy surfaces for partial agonists would likely be quite different (Table 2).

An instructive way to interpret this model is to imagine all of the receptors initially in the resting closed state at the moment of a change in agonist and/or PAM concentration, which will progressively take the receptors through the various levels of agonist occupancy. The top row of schematics illustrates the energy landscape and state transitions for α7 nAChR at various levels of ACh binding in the absence of PNU-120596. Transition from C to the short-lived open state characteristic of α7 (O*) will never occur at high probability, but will be most likely to occur prior to saturation of the agonist binding sites. The energy well for the O* open state in the model is very shallow, consistent with the brief and isolated openings recorded in the outside-out patch experiments (Figure 2). The stability of the D_s and D_i states relative to C increases with

Molecular Pharmacology Fast Forward. Published on September 1, 2011 as DOI: 10.1124/mol.111.074302
This article has not been copyedited and formatted. The final version may differ from this version.

agonist occupancy, and the equilibrium between D_s and D_i will most strongly favor D_i at the highest levels of agonist and PAM occupancy.

Single-channel openings evoked by ACh in the presence of PNU-120596 can occur as extremely long bursts or groups of openings separated by very short closures. This type of activity can be associated with the existence of a long-lived open state(s) (O'). We believe the D_s state represents the rapid concentration-dependent form of desensitization unique to α7, and we hypothesize that PNU-120596 converts or connects the D_s state into the O' state(s). Note that for simplicity only one O' state is represented in the model; however, our burst analysis suggests that the O' states may be kinetically distinct at different levels of agonist and PAM occupancy. We hypothesize that the short intraburst closures, many of which appear as subconductances, represent the reverberation between D_s and O' in the presence of PNU-120596. The O' state(s) may be analogous to the long-lived open states of doubly liganded heteromeric receptors so that conversions between D_s to O' are the primary mechanism through which PNU-120596 reconciles the peak current and net charge ACh concentration-response curves of α7 receptors (Figure 1). Entry into D_i states primarily occurs through activated channel states, and the barrier heights between O'/D_s and D_i states are reduced at high occupancy levels. Therefore, strong ion channel activation promotes D_i, and a primary effect of high PAM occupancy is to stabilize D_i. The stabilization of D_i by high levels of both agonist and PAM occupancy results in a window where maximal potentiation occurs within the low-intermediate range of both agonist and PAM occupancy.

Molecular Pharmacology Fast Forward. Published on September 1, 2011 as DOI: 10.1124/mol.111.074302
This article has not been copyedited and formatted. The final version may differ from this version.

Discussion

The initial characterizations of the type II PAMs PNU-120596, 3a,4,5,9b-Tetrahydro-4-(1-naphthalenyl)-3*H*-cyclopentan[*c*]quinoline-8-sulfonamide (TQS), and 4-(5-(4-chlorophenyl)-2-methyl- 3-propionyl-1*H*-pyrrol-1-yl)benzenesulfonamide (A-867744) reported that these agents reverse or eliminate desensitization (Williams et al., 2011b). Our results show that at least two distinct forms of α7 desensitization exist based on their stability in the presence of PNU-120596. The published literature lacks a formal description of D_i, but there are some published observations from other research groups that we interpret as consistent with the existence of PAM-insensitive D_i states. First, when agonist concentrations are increased in the presence of a fixed PAM concentration, responses are generally enhanced over the full agonist concentration ranges, but the magnitude of potentiation often tends to peak at intermediate concentrations and actually decrease at the higher agonist concentrations (Dinklo et al., 2011; Gronlien et al., 2007; Hurst et al., 2005). A similar phenomenon is sometimes observed when modulator concentrations are increased in the presence of a constant agonist concentration (Dinklo et al., 2011; Dunlop et al., 2009). Second, applications of TQS (Gronlien et al., 2007) or A-867744 (Malysz et al., 2009) were shown to re-activate receptors that had been desensitized by a high concentration of agonist and produced a non-decaying current on the time scale of the experiments, consistent with reversal of D_s states to O' states. However, the peak of the potentiated current in the presence of either TQS or A-867744 was only ~50% of the peak response recorded in the absence of PAM, indicating that only a fraction of the receptor populations were actually conducting current at any given moment. Third, several applications of 30 μM nicotine, with short inter-stimulus intervals, in the continued presence of PNU-120596 produced successively smaller responses (Ng et al., 2007), indicative of the accumulation of modulator-insensitive D_i states. Fourth, an α-bungarotoxin-sensitive and PNU-120596-dependent increase in calcium response from bovine chromaffin cells was only observed when low

Molecular Pharmacology Fast Forward. Published on September 1, 2011 as DOI: 10.1124/mol.111.074302
This article has not been copyedited and formatted. The final version may differ from this version.

(1 μM) concentrations of nicotine were used to stimulate the cells. At concentrations of ≥ 3 μM nicotine, neither PNU-120596 nor α-bungarotoxin had an effect on the response, indicating that the α7 component was lost by the higher nicotine concentrations (del Barrio et al., 2011). In addition, when the α7 component of the total calcium response was isolated, increased concentrations of the α7 agonist *N*-(3*R*)-1-Azabicyclo[2.2.2]oct-3-yl-4-chlorobenzamide (PNU-282987) with a fixed PNU-120596 concentration resulted in decreased α7-dependent calcium responses (del Barrio et al., 2011).

The truly dynamic nature of the interacting effects of agonist and PNU-120596 over time are illustrated by the long bath application responses showing biphasic currents. Biphasic currents have also been reported in currents potentiated by TQS (Gronlien et al., 2007; Malysz et al., 2009). There are numerous factors contributing to these responses, which are difficult to tease apart. The receptors are initially assumed to be in the unliganded resting closed state, with agonist binding occurring as functions of the solution exchange rate and the agonist concentration applied. Our data suggest that PNU-120596 binding occurs more slowly than ACh binding, but is cooperatively influenced by channel activation since the onset of PNU-120596 potentiation occurs more rapidly with strong receptor stimulation by agonist. Interestingly, the transient peak currents are smaller and occur faster with increasing concentrations of ACh and PNU-120596, suggesting that a limiting process is increased by both of these factors (Papke, 2009). It seems reasonable to hypothesize this limiting factor is D_i. We further hypothesize that an immediate effect of PNU-120596 may be to lower the energy barriers for agonist-evoked activation, with relatively little initial effect on desensitization, and that the steady-state currents develop over time as PNU-120596 converts D_s states into O' states and alters the relative free energy levels and establishes a new equilibrium between non-conducting D_i and conducting D_s/O' states. Interestingly, our data suggest that competitive antagonists may influence the equilibrium established between D_s and D_i during prolonged agonist and PNU-120596 applications to produce either positive or

Molecular Pharmacology Fast Forward. Published on September 1, 2011 as DOI: 10.1124/mol.111.074302
This article has not been copyedited and formatted. The final version may differ from this version.

negative effects, depending on agonist concentration. Notably, competitive antagonists appeared to have the effect of shifting the equilibrium in favor of D_s and activatible states when agonist concentration and, by inference, agonist occupancy was high.

The strong apparent induction of D_i in the outside-out patches, yet with extremely long bursting activity of individual channels, suggests PNU-120596 is capable of having very large effects on just a few channels at a time. While the net charge of an oocyte whole-cell current is increased as much as 500-fold by PNU-120596, the net charge of a single-channel burst for a PNU-120596-primed channel is approximately 100,000 times greater than that of a non-potentiated α7 single-channel opening. These two numbers are resolved if only 1 in 200 receptors are active in the bursting states at any moment during a PNU-120596 treatment. While our data suggest that high levels of agonist occupancy generally disfavor channel opening through stabilization of D_i, the mode by which a few resilient PNU-120596-primed channels escape D_i and enter the hyper-bursting state, despite high agonist and PAM occupancy, is less clear. These observations indicate that PNU-120596-primed currents should be used with caution for setting a lower-limit on N, meaning the α7 P_{open} estimate following application of 60 μM ACh could be much less than 7.4×10^{-6}. Even if this upper-limit is greatly overestimated, the data in Figure 2 argue strongly against the assumption that α7 P_{open} is high immediately following rapid exposure to agonist, as previously proposed (Bouzat et al., 2008).

The observation that bursting activity of single-channels in the presence of PNU-120596 persists for approximately 2.5 seconds after removal of external ACh is consistent with the prolonged retention of ACh once channels enter the PNU-120596-primed bursting mode. This observation, in combination with the finding that the onset of potentiation by PNU-120596 is dependent on channel activity, suggests the possibility that agonist and PAM binding sites mutually interact. This possibility is supported by a recent report that the potency of the agonist PNU-282987 to evoke calcium responses in IMR-32 cells was increased with higher PNU-120596 concentrations, and, vice versa, the

Molecular Pharmacology Fast Forward. Published on September 1, 2011 as DOI: 10.1124/mol.111.074302
This article has not been copyedited and formatted. The final version may differ from this version.

potency of PNU-120596 to potentiate responses was increased with higher PNU-282987 concentrations (Gopalakrishnan et al., 2011). In addition, computer docking simulations predicted that binding of PNU-120596 to the proposed transmembrane cavity has higher affinity in an "open" channel model than in a "closed" channel model (Young et al., 2008).

Activation of α7 can have either protective or toxic effects depending on the mode of stimulation (Li et al., 1999), and the potential for enormous potentiation of α7 responses by type II PAMs invites the concern that potentiation of α7 with type II PAMs may bring receptor activation to dangerously high levels (reviewed in (Williams et al., 2011b). There are contradicting reports in the published literature regarding the *in vitro* cytotoxicity profile of PNU-120596; in the two cases where PNU-120596 was found to be toxic (Dinklo et al., 2011; Ng et al., 2007), the stimulating agonist was the weakly potent α7 agonist choline at a concentration of ~100 μM, which is well below the published EC_{50} value (Papke and Papke, 2002) and potentially falls within the window of strong α7 potentiation where D_i is avoided. In contrast, PNU-120596 was reported to lack a significant cytotoxicity profile when co-applied with 10 μM of the potent α7 agonist PNU-282987 (Hu et al., 2009). Given that the published EC_{50} value of PNU-282987 in the presence of 3 μM PNU-120596 is ~200 nM (Gronlien et al., 2007), and D_i induced by high PNU-282987 concentrations is apparent in bovine chromaffin cells (del Barrio et al., 2011), the existence of D_i states, which may provide an intrinsic safety mechanism, might account for the lack of toxicity in this study and for the discrepancy in the published literature regarding type II PAM toxicity profiles.

Our data indicate that even for the structurally related benzylidene anabaseine compounds there are significant equilibrium energy differences associated with the D_s and D_i states. Molecular docking studies of the benzylidene anabaseine compounds suggest that the benzylidene group extends into the intersubunit interface (Horenstein et al., 2007), and our data would suggest that specific point-to-point interactions between

Molecular Pharmacology Fast Forward. Published on September 1, 2011 as DOI: 10.1124/mol.111.074302
This article has not been copyedited and formatted. The final version may differ from this version.

sidegroups on the benzylidene and specific amino acid residues in the cleft may be exploited to differentially stabilize receptors in the D_s and D_i states. The structure of the acetylcholine binding protein bound with diMeOBA, the compound which most effectively induced D_i or other nonresponsive states, showed that the molecule might be bound in entirely different orientations at the various subunit interfaces (Hibbs et al., 2009). In addition, recent work with tethered agonists has shown that a single ligand molecule may bind the ligand binding domain in different orientations, each of which may differentially affect activation and desensitization (Wang et al., 2010). Identification of compounds that preferentially stabilize specific functional states, including D_s and D_i, may be therapeutically important if it can be shown that a specific state is important for signal transduction attributed to α7. Interestingly, α7-mediated signal transduction has been observed under conditions when ion channel activation is not apparent (Skok, 2009), leaving the intriguing possibility open that α7 desensitized states are not inactive, but functionally meaningful.

Molecular Pharmacology Fast Forward. Published on September 1, 2011 as DOI: 10.1124/mol.111.074302
This article has not been copyedited and formatted. The final version may differ from this version.

Acknowledgements

We thank Dr. F. Soti (University of Florida, Department of Pharmacology and Therapeutics) for helpful advice on the synthesis of PNU-120 596, Clare Stokes for editorial comments, and Dr. Nicole Horenstein for numerous helpful discussions. OpusXpress experiments were conducted by Shehd Abdullah Abbas Al Rubaiy, Sara Copeland, Matthew Kimbrell, and Clare Stokes. The L9'T mutant of the human α7 was made by Clare Stokes. We thank Dr. Lynn Wecker (University of South Florida) for the use of an additional OpusXpress 6000.

Molecular Pharmacology Fast Forward. Published on September 1, 2011 as DOI: 10.1124/mol.111.074302
This article has not been copyedited and formatted. The final version may differ from this version.

Authorship Contributions

Participated in research design: Papke and Williams

Conducted experiments: Williams

Contributed reagents or analytic tools: Wang

Performed data analysis: Williams and Papke

Wrote or contributed to the writing of the manuscript: Williams, Wang, and Papke

References

Bertrand S, Devillers-Thiery A, Palma E, Buisson B, Edelstein SJ, Corringer PJ, Changeux JP and Bertrand D (1997) Paradoxical allosteric effects of competitive inhibitors on neuronal alpha7 nicotinic receptor mutants. Neuroreport 8(16):3591-3596.

Bouzat C, Bartos M, Corradi J and Sine SM (2008) The interface between extracellular and transmembrane domains of homomeric Cys-loop receptors governs open-channel lifetime and rate of desensitization. J Neurosci 28(31):7808-7819.

Colquhoun D and Sakmann B (1985) Fast events in single-channel currents activated by acetylcholine and its analogues at the frog muscle end-plate. Journal of Physiology (London) 369:501-557.

Colquhoun D and Sakmann B (1995) Fitting and statistical analysis of single-channel records., in Single-Channel Recording (Sakmann B and Neher E eds) pp 483-585, Plenum Press, New York, NY.

del Barrio L, Egea J, Leon R, Romero A, Ruiz A, Montero M, Alvarez J and Lopez MG (2011) Calcium signalling mediated through alpha7 and non-alpha7 nAChR stimulation is differentially regulated in bovine chromaffin cells to induce catecholamine release. Br J Pharmacol 162(1):94-110.

Dinklo T, Shaban H, Thuring JW, Lavreysen H, Stevens KE, Zheng L, Mackie C, Grantham C, Vandenberk I, Meulders G, Peeters L, Verachtert H, De Prins E and Lesage AS (2011) Characterization of 2-[[4-fluoro-3-(trifluoromethyl)phenyl]amino]-4-(4-pyridinyl)-5-thiazolemethanol (JNJ-1930942), a novel positive allosteric modulator of the {alpha}7 nicotinic acetylcholine receptor. J Pharmacol Exp Ther 336(2):560-574.

Dunlop J, Lock T, Jow B, Sitzia F, Grauer S, Jow F, Kramer A, Bowlby MR, Randall A, Kowal D, Gilbert A, Comery TA, Larocque J, Soloveva V, Brown J and Roncarati R (2009) Old and new pharmacology: positive allosteric modulation of the alpha7 nicotinic acetylcholine receptor by the 5-hydroxytryptamine(2B/C) receptor antagonist SB-206553 (3,5-dihydro-5-methyl-N-3-pyridinylbenzo[1,2-b:4,5-b']di pyrrole-1(2H)-carboxamide). J Pharmacol Exp Ther 328(3):766-776.

Gopalakrishnan SM, Philip BM, Gronlien JH, Malysz J, Anderson DJ, Gopalakrishnan M, Warrior U a nd Burns DJ (2011) Functional Characterization and Hi gh-Throughput Screening of Positive Allosteric Modulators of alpha7 Nicotinic Acetylcholine Receptors in IMR-32 Neuroblastoma Cells. Assay Drug Dev Technol. Online Ahead of Print: February 10, 2011

Gronlien JH, Haakerud M, Ween H, Thorin-Hagene K, Briggs CA, Gopalakrishnan M and Malysz J (2007) Distinct profiles of α7 nAChR positive allosteric modulation revealed by structurally diverse chemotypes. Mol Pharmacol 72(3):715-724.

Halevi S, McKay J, Palfreyman M, Yassin L, Eshel M, J orgensen E and T reinin M (2002) The C. elegans ric-3 gene is required for ma turation of nic otinic acetylcholine receptors. EMBO J 21(5):1012-1020.

Heidmann T and Changeux JP (1978) Structural and functional properties of the acetylcholine receptor protein in its purified and membrane-bound states. Annu Rev Biochem 47:317-357.

Hibbs RE, Sulzenbacher G, Shi J, Talley TT, Conrod S, Kem WR, Taylor P, Marchot P and Bourne Y (2009) Structural determinants for interaction of partial agonists with acetylcholine binding protein and neuronal alpha7 nicotinic acetylcholine receptor. EMBO J 28(19):3040-3051.

Horenstein NA, McCormack TJ, Stokes C, Ren K and Papke RL (2007) Reversal of agonist selectivity by mutations of conserved amino acids in the binding site of nicotinic acetylcholine receptors. J Biol Chem 282(8):5899-5909.

Hu M, Gopalakrishnan M and Li J (2009) Positive allosteric modulation of alpha7 neuronal nicotinic acetylcholine receptors: lack of cytotoxicity in PC12 cells and rat primary cortical neurons. Br J Pharmacol 158(8):1857-1864.

Hurst RS, Hajos M, Raggenbass M, Wall TM, Higdon NR, Lawson JA, Rutherford-Root KL, Berkenpas MB, Hoffmann WE, Piotrowski DW, Groppi VE, Allaman G, Ogier R, Bertrand S, Bertrand D and Arneric SP (2005) A novel positive allosteric modulator of the alpha7 neuronal nicotinic acetylcholine receptor: in vitro and in vivo characterization. J Neurosci 25(17):4396-4405.

Lape R, Colquhoun D and Sivilotti LG (2008) On the nature of partial agonism in the nicotinic receptor superfamily. Nature 454(7205):722-727.

Li Y, Papke RL, He Y-J, Millard B and Meyer EM (1999) Characterization of the neuroprotective and toxic effects of α7 nicotinic receptor activation in PC12 cells. Brain Res 81(4):218-225.

Malysz J, Gronlien JH, Anderson DJ, Hakerud M, Thorin-Hagene K, Ween H, Wetterstrand C, Briggs CA, Faghih R, Bunnelle WH and Gopalakrishnan M (2009) In vitro pharmacological characterization of a novel allosteric modulator of alpha 7 neuronal acetylcholine receptor, 4-(5-(4-chlorophenyl)-2-methyl-3-propionyl-1H-pyrrol-1-yl)benzenesulfonamide (A-867744), exhibiting unique pharmacological profile. J Pharmacol Exp Ther 330(1):257-267.

McNerney ME, Pardi D, Pugh PC, Nai Q and Margiotta JF (2000) Expression and channel properties of alpha-bungarotoxin-sensitive acetylcholine receptors on chick ciliary and choroid neurons. J Neurophysiol 84(3):1314-1329.

Mike A, Castro NG and Albuquerque EX (2000) Choline and acetylcholine have similar kinetic properties of activation and desensitization on the alpha7 nicotinic receptors in rat hippocampal neurons. Brain Res 882(1-2):155-168.

Millar NS and Gotti C (2009) Diversity of vertebrate nicotinic acetylcholine receptors. Neuropharmacology 56(1):237-246.

Ng HJ, Whittemore ER, Tran MB, Hogenkamp DJ, Broide RS, Johnstone TB, Zheng L, Stevens KE and Gee KW (2007) Nootropic alpha7 nicotinic receptor allosteric modulator derived from GABAA receptor modulators. Proc Natl Acad Sci U S A 104(19):8059-8064.

Palma E, Bertrand S, Binzoni T and Bertrand D (1996) Neuronal nicotinic alpha 7 receptor expressed in Xenopus oocytes presents five putative binding sites for methyllycaconitine. J Physiol 491(Pt 1):151-161.

Papke RL (1993) Use-dependent inhibition of neuronal nicotinic ACHR by Tinuvin® 770 (BIS (2, 2, 6, 6, - Tetramethyl-4-Piperidinyl) Sebacacate), a possible additive to laboratory plastics, in Biophy J pp W-pos421.

Papke RL (2009) Tricks of Perspective: Insights and limitations to the study of macroscopic currents for the analysis of nAChR activation and desensitization. Journal of Molecular Neuroscience 40(1-2):77-86.

Papke RL, Dwoskin LP, Crooks PA, Zheng G, Zhang Z, McIntosh JM and Stokes C (2008) Extending the analysis of nicotinic receptor antagonists with the study of alpha6 nicotinic receptor subunit chimeras. Neuropharmacology 54(8):1189-1200.

Papke RL, Kem WR, Soti F, López-Hernández GY and Horenstein NA (2009) Activation and desensitization of nicotinic alpha7-type acetylcholine receptors by benzylidene anabaseines and nicotine. J Pharmacol Exp Ther 329(2):791-807.

Papke RL, Meyer E, Nutter T and Uteshev VV (2000) Alpha7-selective agonists and modes of alpha7 receptor activation. Eur J Pharmacol 393(1-3):179-195.

Papke RL and Papke JKP (2002) Comparative pharmacology of rat and human alpha7 nAChR conducted with net charge analysis. Br J of Pharm 137(1):49-61.

Papke RL, Schiff HC, Jack BA and Horenstein NA (2005) Molecular dissection of tropisetron, an alpha7 nicotinic acetylcholine receptor-selective partial agonist. Neurosci let 378:140-144.

Papke RL and Stokes C (2010) Working with OpusXpress: methods for high volume oocyte experiments. Methods 51(1):121-133.

Papke RL and Thinschmidt JS (1998) The correction of alpha7 nicotinic acetylcholine receptor concentration-response relationships in *Xenopus* oocytes. Neurosci Let 256:163-166.

Piotrowski DW, Rogers BN, McWhorter WW, Jr., Walker DP, Corbett JW, Groppi VE, Jr. and Rudmann DG (2003) Preparation of ureas as positive allosteric modulators of the nicotinic acetylcholine receptor, Patent, Pharmacia & Upjohn Company, April 28, 2003, WO2003093250A2, 13 Nov 2003.

Placzek AN, Grassi F, Meyer EM and Papke RL (2005) An alpha7 nicotinic acetylcholine receptor gain-of-function mutant that retains pharmacological fidelity. Mol Pharmacol 68(6):1863-1876.

Qin F (2004) Restoration of single-channel currents using the segmental k-means method based on hidden Markov modeling. Biophys J 86(3):1488-1501.

Skok MV (2009) To channel or not to channel? Functioning of nicotinic acetylcholine receptors in leukocytes. J Leukoc Biol 86(1):1-3.

Wang J, Horenstein NA, Stokes C and Papke RL (2010) Tethered agonist analogs as site-specific probes for domains of the human alpha7 nicotinic acetylcholine receptor that differentially regulate activation and desensitization. Mol Pharmacol 78(6):1012-1025.

Williams DK, Stokes C, Horenstein NA and Papke RL (2011a) The effective opening of nicotinic acetylcholine receptors with single agonist binding sites. J Gen Physiol 137(4):369-384.

Williams DK, Wang J and Papke RL (2011b) Positive allosteric modulators as an approach to nicotinic acetylcholine receptor-targeted therapeutics: Advantages and limitations. Biochem Pharmacol 82(8):915-30.

Young GT, Zwart R, Walker AS, Sher E and Millar NS (2008) Potentiation of alpha7 nicotinic acetylcholine receptors via an allosteric transmembrane site. Proc Natl Acad Sci U S A 105(38):14686-14691.

Zhou Y, Nelson ME, Kuryatov A, Choi C, Cooper J and Lindstrom J (2003) Human alpha4beta2 acetylcholine receptors formed from linked subunits. J Neurosci 23(27):9004-9015.

Molecular Pharmacology Fast Forward. Published on September 1, 2011 as DOI: 10.1124/mol.111.074302
This article has not been copyedited and formatted. The final version may differ from this version.

Footnotes

This work was supported by National Institute of Hea lth grants [RO1-GM57481] and [T32-AG000196].

The original document describing synthesis of PNU-120596-related compounds can be found at http://www.wipo.int/patentscope/search/en/WO2003093250.

Molecular Pharmacology Fast Forward. Published on September 1, 2011 as DOI: 10.1124/mol.111.074302
This article has not been copyedited and formatted. The final version may differ from this version.

Legends for Figures

Figure 1. The basic characterization of α7 macroscopic currents, comparison to currents from heteromeric α4β2 nAChR, and the effects of PNU-120596. **A)** Displayed in the upper panel are recordings from a *Xenopus* oocyte expressing human α4β2 nAChR to the application of a range of ACh concentrations. Receptors with a fixed subunit stoichiometry of three α4 and two β2 were obtained by co-expressing a concatamer of β2 and α4 (β2–6–α4, (Zhou et al., 2003)) with monomeric α4. In the lower panel are the average values for peak currents and net charge for the ACh-evoked responses of α4β2 expressing oocytes. The EC_{50} values for peak and net charge measurements were 157±28 μM and 184±25 μM, respectively. Each point is the average of at least 4 cells ± SEM. **B)** Displayed in the upper panel are recordings from a *Xenopus* oocyte expressing human α7 nAChR to the application of a range of ACh concentrations. In the lower panel are the average values for peak currents and net charge for the ACh-evoked responses of α7-expressing oocytes. The EC_{50} values for peak and net charge measurements were 311±15 μM and 98±12 μM, respectively. Each point is the average of at least 4 cells ± SEM. **C)** Displayed in the upper panel are recordings from a *Xenopus* oocyte expressing human α7 nAChR to the application of a range of ACh concentrations obtained in the presence of 10 μM PNU-120596, compared to an initial control response 60 μM ACh alone from the same oocyte. In the lower panel are the average values for peak currents and net charge of α7-expressing oocytes for the ACh-evoked responses in 10 μM PNU-120596. The EC_{50} values for peak and net charge measurements were 48±6 μM and 49±7 μM, respectively. Each point is the average of at least 4 cells ± SEM. After obtaining two initial control responses to the application of 60 μM ACh alone, the bath perfusion system was switched to a solution of Ringer's plus 10 μM PNU-120596. ACh applications were made with the pipette delivery system. ACh solutions were made up in

Molecular Pharmacology Fast Forward. Published on September 1, 2011 as DOI: 10.1124/mol.111.074302
This article has not been copyedited and formatted. The final version may differ from this version.

the PNU-120596-containing bath solution. Net charge responses were calculated for a period of 120 s following the initiation of drug applications.

Figure 2. The low intrinsic P_{open} of α7 is enhanced by PNU-120596. Data were obtained from outside-out patches pulled from BOSC 23 cells transiently expressing human α7 and RIC-3. **A)** A typical response evoked by rapid (≤0.7 ms) application of 60 μM ACh showing the short-lived openings that are characteristic of α7. Notice that the frequency of channel openings quickly diminishes following exposure of the patch to ACh. **B)** A histogram of the apparent single-channel α7 open durations evoked by 60 μM ACh (n = 187 open events from 13 patches; 10 kHz bandwidth). Putative openings that could not be clearly distinguished from brief, random noise spikes were excluded from the histogram. The histogram is described by a single exponential function, which predicts that α7 single-channel openings are, on average, approximately 60 μs in duration, assuming that the distribution of openings too short to be detected (<40 μs) reasonably follows the fit exponential function. **C)** Responses produced by 60 μM ACh and relative increases produced with co-application of with 60 μM ACh and 10 μM PNU-120596. Drug applications and inter-stimulus intervals were 12 s and 30 s in duration, respectively.

Figure 3. PNU-120596 operates on the same population of receptors that are activatible in the absence of the PAM. In order to determine whether PNU-120596 increases the number of activatible receptors, we determined the effects of the slowly reversible use-dependent inhibitor BTMPS (Papke, 1993) with or without the potentiating effects of PNU-120596. **A)** Sample traces illustrating the slow recovery of responses evoked by 60 μM ACh following a single co-application of ACh with 100 μM BTMPS. Responses in the upper trace were obtained without PNU-120596. The lower two traces illustrate the effect of a single co-application of PNU-120596 with or without a preceding co-

Molecular Pharmacology Fast Forward. Published on September 1, 2011 as DOI: 10.1124/mol.111.074302
This article has not been copyedited and formatted. The final version may differ from this version.

application of ACh and BTMPS. **B)** Average data for the effect of BTMPS on the responses of at least 4 oocytes (± SEM) obtained 8 minutes after a co-application of ACh and the antagonist. Data obtained without PNU-120596 were normalized to the initial ACh-evoked responses. Data obtained from cells treated with both BTMPS and PNU-120596 went through a two-step normalization. Each cell's responses were first calculated relative to the initial ACh controls from the same cells. The responses to ACh plus PNU-120596 in the BTMPS-treated cells were then expressed relative to the average potentiation obtained in the cells treated with PNU-120596 without prior treatment with BTMPS.

Figure 4. Convergence and competition of type I and type II PAM activity and PAM effects on "gain-of-function" mutants. **A)** Competitive effects of the prototypical type I PAM 5HI on the potentiation of 60 μM ACh evoked responses of oocytes expressing human α7 nAChR. After obtaining control responses to 60 μM ACh, responses were obtained to co-applications of ACh plus 1 mM 5HI, 10 μM PNU-120596, or the two PAMs in combination. Data are the averages of at least 4 oocytes (±SEM) for each condition. The co-application of 5HI with PNU-120596 produced significantly less ($p < 0.05$) potentiation than that produced with PNU-120596 alone. **B)** Representative traces illustrating the effects of two gain-of-function mutations in the second transmembrane domain of α7 nAChR. The effects of the T6'S mutation (Placzek et al., 2005) are qualitatively similar to those of type 1 PAMs, while the effects of the well-studied L9'T mutation are greater (Bertrand et al., 1997), especially in regard to the characteristic rapid desensitization of α7, and have been compared to the effects of a type II PAM (Gronlien et al., 2007). **C)** The effects of the T6'S and L9'T mutations on the activity of the type I PAM 5HI. Although, as expected, the ACh control responses of α7T6'S receptors were larger than the responses of wild-type α7 receptors, the effects of 5HI pre- and co-applications were relatively similar to effects on wild-type receptors. In contrast, α7L9'T

Molecular Pharmacology Fast Forward. Published on September 1, 2011 as DOI: 10.1124/mol.111.074302
This article has not been copyedited and formatted. The final version may differ from this version.

responded to the pre-application of 5HI alone, and responses during the co-application of 5HI and ACh were smaller than to ACh alone. **D)** The effects of the T6'S and L9'T mutations on the activity of the type II PAM PNU-120596. Although, as expected, the ACh control responses of α7T6'S receptors were larger than the responses of wild-type α7 receptors, the effects of PNU-120596 pre- and co-applications were relatively similar to effects on wild-type receptors. In contrast, α7L9'T responded to the pre-application of PNU-120596 alone, and responses during the co-application of PNU-120596 and ACh were smaller than to ACh alone. In all traces (panels B-D) the black bars represent 20 s applications of 60 μM ACh.

Figure 5. Factors defining and limiting the potentiating effects of PNU-120596 on α7 nAChR expressed in *Xenopus* oocytes. **A)** Maximum potentiation of 60 μM ACh-evoked responses obtained with different concentrations of bath-applied PNU-120596 applied repeatedly at 4-minute intervals for over 60 minutes. **B)** The time course of the potentiation of 60 μM ACh-evoked responses by varying concentrations of bath-applied PNU-120596. Note that although each point represents the average of at least four oocytes, error bars have been omitted for clear presentation of the kinetic differences. In the presence of 0.3 μM PNU-120596, potentiation was significantly ($p < 0.01$) larger at 64 minutes than at 12 minutes. In the presence of 1.0 μM PNU-120596, potentiation was greater at 40 minutes than at 12 minutes ($p < 0.05$), but not significantly greater at 64 minutes than at 12 minutes. For all concentrations of PNU-120596 $\geq$ 3 μM, the potentiation at 64 minutes was significantly less than that at 12 minutes ($p < 0.05$).

Figure 6. Agonist concentration dependence on the onset and decline of potentiation by PNU-120596 in outside-out patches containing α7 receptors. Comparison of responses from the same patch potentiated by 10 μM PNU-120596 and evoked by 1 μM ACh or 100 μM ACh. Drug applications and inter-stimulus intervals were 45 s and 55 s in

duration, respectively. The ensemble average of all four current traces was created by first normalizing each data point of an individual trace to the peak current of that trace. Then, the average value of the normalized currents was calculated for each data point.

Figure 7. Activity dependence of potentiation onset and decline in *Xenopus* oocytes. **A)** Representative raw data showing the repeated stimulation of α7-expressing oocytes in the presence of 3 μM PNU-120596. Cells were either stimulated repeatedly with 10 μM ACh (upper trace), or 10 μM ACh alternating with applications of 300 μM ACh (lower trace). **B)** Average data (±SEM) for 10 μM ACh-evoked responses obtained with the two protocols illustrated in panel A. Note that maximal potentiation was achieved more rapidly when there were alternating applications of the high concentration of ACh; however, potentiation subsequently declined.

Figure 8. Recovery from PNU-120596 insensitive desensitization (D_i). **A)** *Xenopus* oocytes expressing human α7 were stimulated repeatedly with 60 μM ACh in the presence of 10 μM PNU-120596. The amount of potentiation rapidly reached a maximum and then began to decline. To determine if the decline in ACh-evoked responses represented a reversible form of PNU-120596 desensitization, some cells (solid points) received 6 applications of PNU-120596 solution alone rather than repeated co-applications of ACh plus PNU-120596. Subsequent application of ACh plus PNU-120596 to the cells which had received a respite from the repeated ACh stimulations gave responses that returned to a level that was not different the previously maximal level of potentiation, and significantly greater than ($p < 0.01$) that of the cell receiving continuous stimulation. **B)** Responses from outside-out patches expressing α7 to co-application of 300 μM ACh and 10 μM PNU-120596 show a rapid rise and subsequent decay despite the continued presence of ACh and PNU-120596, indicative of stabilized D_i states. Recovery from D_i induced by co-application of 300 μM ACh and 10 μM PNU-120596

Molecular Pharmacology Fast Forward. Published on September 1, 2011 as DOI: 10.1124/mol.111.074302
This article has not been copyedited and formatted. The final version may differ from this version.

occurs rapidly. Identical 45 s drug applications were separated by 5 s inter-stimulus intervals.

Figure 9. Single-channel α7 bursts evoked by 300 μM ACh and potentiated by 10 μM PNU-120596. **A)** Continuous data demonstrating the bursting characteristics and high steady-state P_{open} of single-channel openings potentiated by PNU-120596. **B)** Fit histograms displaying apparent open durations from α7 channels activated by 300 μM ACh and potentiated by 10 μM PNU-120596. Shown are histograms compiled from currents potentiated by PNU-120596 that occur as brief events in isolation, and in long groups of openings as bursts. Two classes of bursts are distinguished based on the average intraburst open duration, which is demonstrated below with a scatter plot of average intraburst duration versus total burst length. **C)** PNU-120596-potentiated channel openings persist for seconds after removal of external ACh. Left, an example of a protracted macroscopic current that persisted for approximately 8.3 seconds after external ACh removal. Right, single-channel bursts showing protracted currents of various durations after external ACh removal. **D)** The protracted currents were not an artifact of solution exchange. Above, solution exchanges typically occurred within 400 - 700 μs, as measured by open-tip recordings performed following data collection from each patch. Below, a sharp reduction in current noise was associated with the removal of external ACh. The noise was likely due to channel block by agonist, which disappeared as external agonist was removed. **E)** Application of the competitive antagonist MLA at 3 μM following removal of external ACh significantly ($p < 1 \times 10^{-5}$) shortened the duration of protracted currents. Both currents displayed in panel E were obtained from the same patch.

Figure 10. Dynamic aspects of α7 nAChR responses to bath application of ACh and PNU-120596. **A)** Representative traces illustrating the response of human α7 nAChR

Molecular Pharmacology Fast Forward. Published on September 1, 2011 as DOI: 10.1124/mol.111.074302
This article has not been copyedited and formatted. The final version may differ from this version.

expressed in *Xenopus* oocytes to the bath application of 3 μM PNU-120596 and various concentration of ACh, as indicated. All responses are scaled relative to each cell's response to a control application of 60 μM ACh (black bar, far left) prior to 30-minute bath applications of ACh and the PAM. **B)** Representative responses to ACh co-applied with either 3 μM or 10 μM PNU-120596. The data for the co-application responses to 10 μM PNU-120596 plus either 30 or 300 μM ACh (gray) are superimposed over the responses to 3 μM PNU-120596 plus either 30 or 300 μM ACh (black), reproduced from panel A. All responses are scaled relative to each cell's response to a control application of 60 μM ACh (black bar, far left). **C)** Time to transient peak current recorded with the co-application of 3 μM PNU-120596 and varying concentrations of ACh. **D)** The amplitude of the transient peak currents (open circles and Y-axis on left) at varying concentrations of ACh in 3 μM PNU-120596 and the fraction of the total net charge in the first 10 minutes of the responses that accumulated during the transient peak (filled circles and Y-axis on right). **E)** Time to transient peak current recorded in the currents shown in panel B. **F)** The net charge in the first 10 minutes of responses obtained under the conditions illustrated in panel B.

Figure 11. Competitive antagonists are active molecules in modulating P_{open} of PNU-primed receptors. **A)** Human α7 nAChR expressed in *Xenopus* oocytes were activated by bath co-application of 3 μm PNU-120596 and varying concentrations of choline as indicated. Varying concentrations of MLA were applied during the co-application responses. As shown in the representative traces, the concentration dependence for MLA effects depended on the concentration of the agonist. In each experiment the MLA applications were followed up by an application of 100 μM of the noncompetitive antagonist mecamylamine to confirm that the large currents were receptor mediated. **B)** Effects of the competitive antagonist DHβE on the responses of human α7 nAChR expressed in *Xenopus* oocytes to co-application of 3 μM PNU-120596 and 200 μM

choline. The effects of DHβE were similar to those of MLA, with a correction for the reduced potency of DHβE compared to MLA for the inhibition of α7 nAChR.

Figure 12. Proposed models for the activation, desensitization, and modulation of α7 nAChR. Shown are qualitative representations of minimal models for α7 nAChR conformational states, their relative energy levels, and transition rates as deduced from our data for varying levels of agonist and PNU-120596 binding. Under equilibrium conditions, the distributions of receptors into the resting closed, open, and desensitized states will be determined by the relative free energy of the states (represented by vertical displacements). Dynamically, the transition rates between the states will be inversely related to the log of the energy barriers between the states. In the absence of any PNU-120596 binding, the primary effect of agonist binding is to shift the equilibrium between the conformational states from the resting closed (C) state toward the desensitized states, D_s, which is sensitive to destabilization by PNU-120596, and D_i, which is insensitive to the activating effects of PNU-120596. The shallow energy well assigned to the open state (O*) is consistent with the brief opening observed in single-channel recordings, and the high energy barriers into the O* state are consistent with the low P_{open} observed. The lower two rows include a new long-lived open state O', promoted by the binding of PNU-120596 and possibly connected to a modified form of the D_s state which is converted to a subconductance.

Tables

Table 1. Fit time-constants from event duration histograms in the presence of 300 μM ACh and 10 μM PNU-120596[a]

Type of event	Isolated openings		Class I bursts		Class II bursts	
	n/a[b]		P ± sem[c]	τ ± sem[d]	P ± sem	τ ± sem
Intraburst closures			0.91 ± 0.06	0.07 ± 0.10	0.77 ± 0.14	0.16 ± 0.18
			0.07 ± 0.04	0.51 ± 0.82	0.21 ± 0.15	0.57 ± 0.61
			0.02 ± 0.03	9.16± 4.52	0.02 ± 0.04	13.2 ± 2.5
	n/a		P ± sem	τ ± sem	P ± sem	τ ± sem
Intraburst subconductances			0.80 ± 0.12	0.08 ± 0.09	0.82 ± 0.07	0.14 ± 0.09
			0.20 ± 0.04	0.40 ± 0.20	0.18 ± 0.09	0.37 ± 0.24
	P ± sem	τ ± sem	P ± sem	τ ± sem	P ± sem	τ ± sem
Openings or Intraburst openings	0.54 ± 0.02	0.12 ± 0.06	--------	----------	--------	----------
	0.30 ± 0.02	0.71 ± 0.11	--------	----------	--------	----------
	0.16 ± 0.02	8.23 ± 0.14	1	5.35 ± 0.02	1	27.25 ± 0.02

[a]Data obtained from outside-out patches pulled from BOSC 23 cells

[b]Not applicable

[c] P values indicate fraction of total events estimated from histogram fit

[d] τ values indicated in μs

Molecular Pharmacology Fast Forward. Published on September 1, 2011 as DOI: 10.1124/mol.111.074302
This article has not been copyedited and formatted. The final version may differ from this version.

Table 2. Induction of D_s by five-minute incubations[a]

Compound	Evoked response[b]	ACh residual	PAM-evoked	D_s induction[c]
1 mM ACh	1.12 ± 0.08	0.01 ± 0.01	32.1 ± 2.3	1
100 μM diOHBA[d]	0.78 ± 0.06	0.01 ± 0.01	13.3 ± 1.56	3
100 μM 4OH2MeOBA	0.61 ± 0.03	0.02 ± 0.01	0.95 ± 0.15	5
10 μM tropisetron	0.61 ± 0.03	0.01 ± 0.01	25.6 ± 2.2	2
100 μM diMeOBA	0.52 ± 0.17	0.03 ± 0.03	2.97 ± 0.38	4
100 μM lobeline	0.07 ± 0.02	0.21 ± 0.06	0.13 ± 0.02	6

[a]Data obtained from *Xenopus* oocytes

[b]All responses are net charge values, normalized to the average net charge in two initial 60 μM ACh applications.

[c]Rank order for the relative effectiveness of each drug for stabilizing receptors in the D_s, state as measured by the ability of PNU-120596 application to stimulate currents of the predesensitized receptors.

[d]diOHBA, 3-(2,4-dihydroxybenzylidene)anabaseine; 4OH2MeOBA, 3-(4-hydroxy, 2-methoxybenzylidene)anabaseine; tropisetron, (1R,5S)-8-methyl-8-azabicyclo[3.2.1]octan-3-yl 1methyl-indole-3-carboxylate; diOHBA, 3-(2,4-dihydroxybenzylidene)anabaseine; diMeOBA, 3-(2,4-dimethoxybenzylidene)anabaseine; lobeline, 2-[6- (2-hydroxy- 2-phenyl- ethyl)- 1-methyl- 2-piperidyl]- 1-phenyl- ethanone;

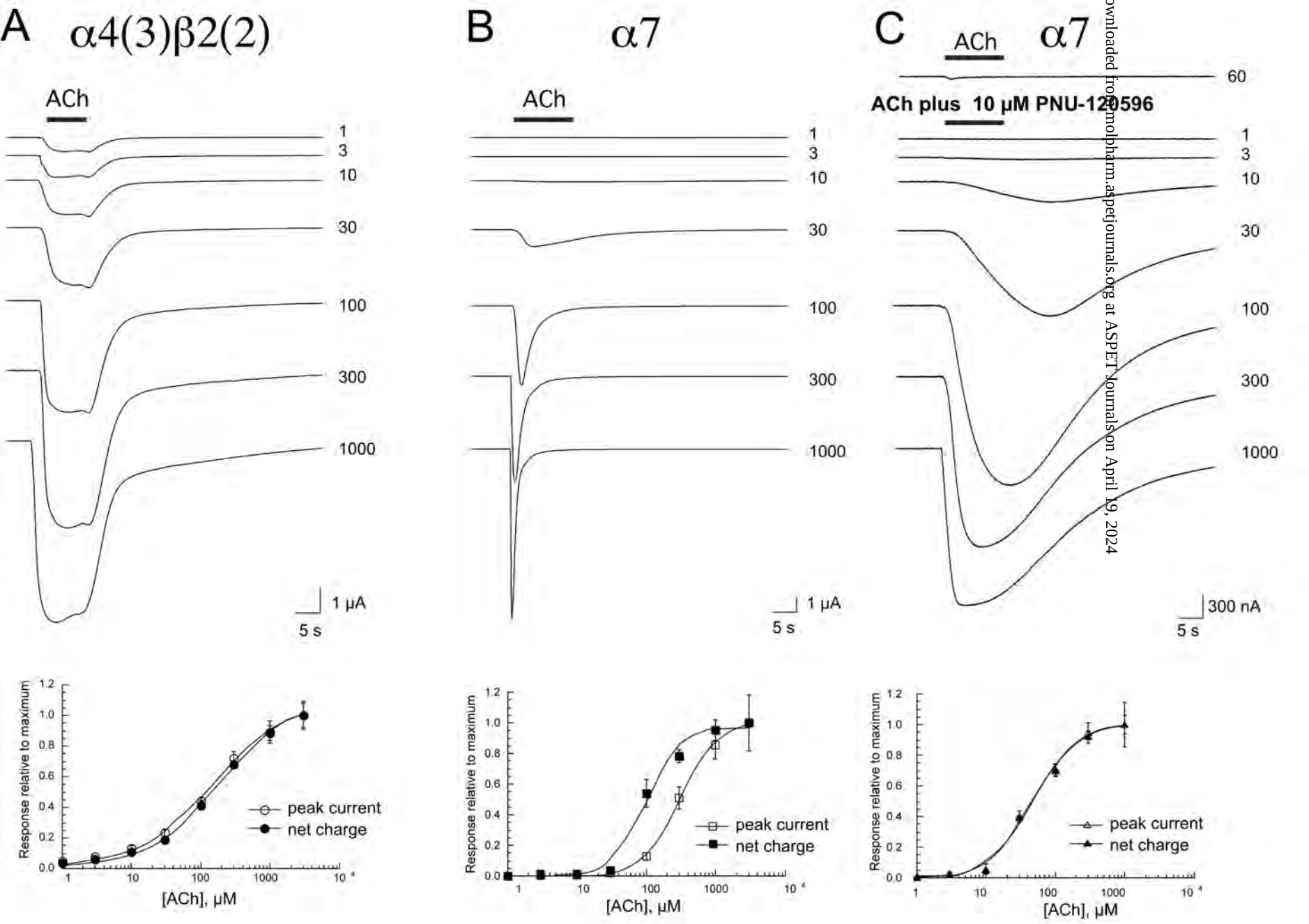

Figure 1

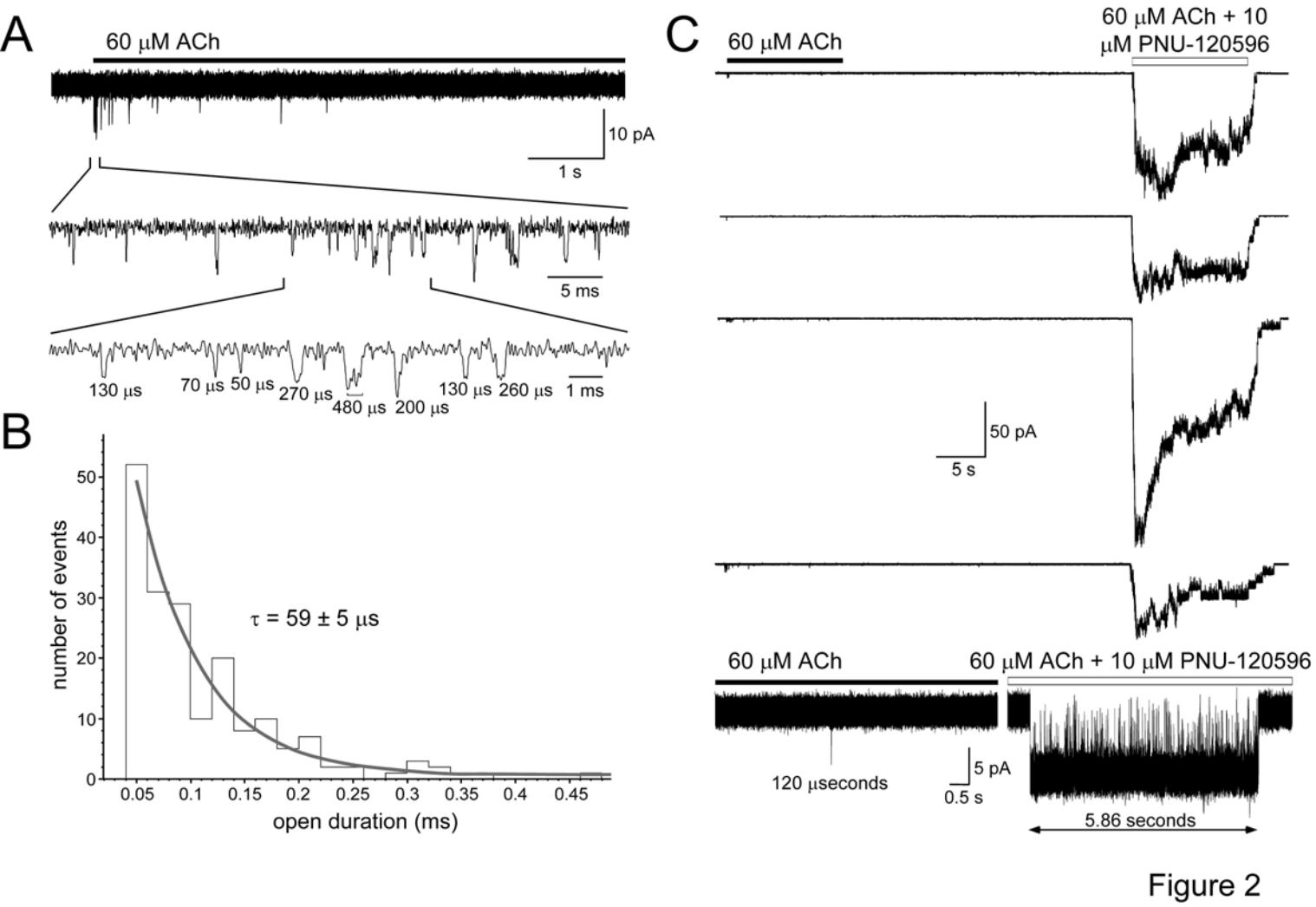
A
60 μM ACh
10 pA
1 s
5 ms
130 μs
70 μs
50 μs
270 μs
480 μs
200 μs
130 μs
260 μs
1 ms
B
number of events
τ = 59 ± 5 μs
open duration (ms)
C
60 μM ACh
60 μM ACh + 10 μM PNU-120596
50 pA
5 s
60 μM ACh
60 μM ACh + 10 μM PNU-120596
120 μseconds
5 pA
0.5 s
5.86 seconds

Figure 2

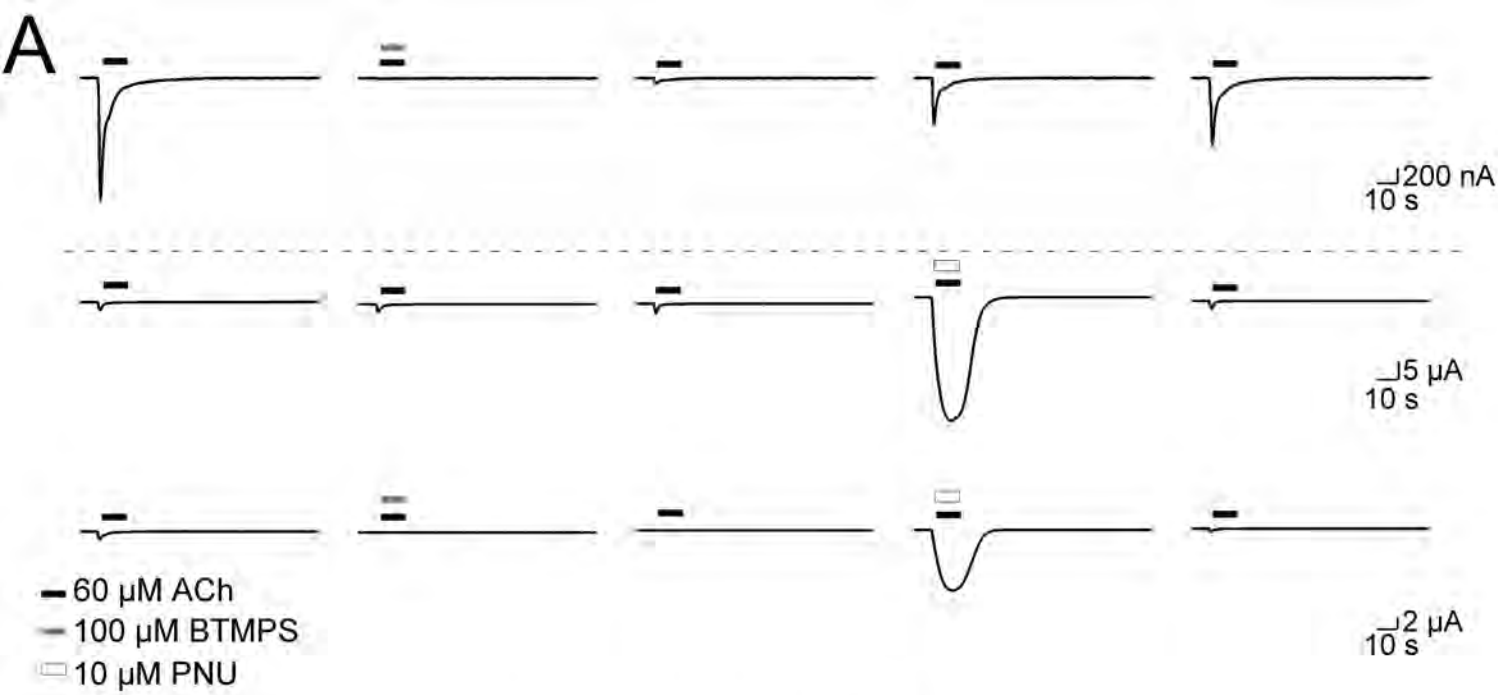
A
200 nA
10 s
5 µA
10 s
2 µA
10 s
60 µM ACh
100 µM BTMPS
10 µM PNU

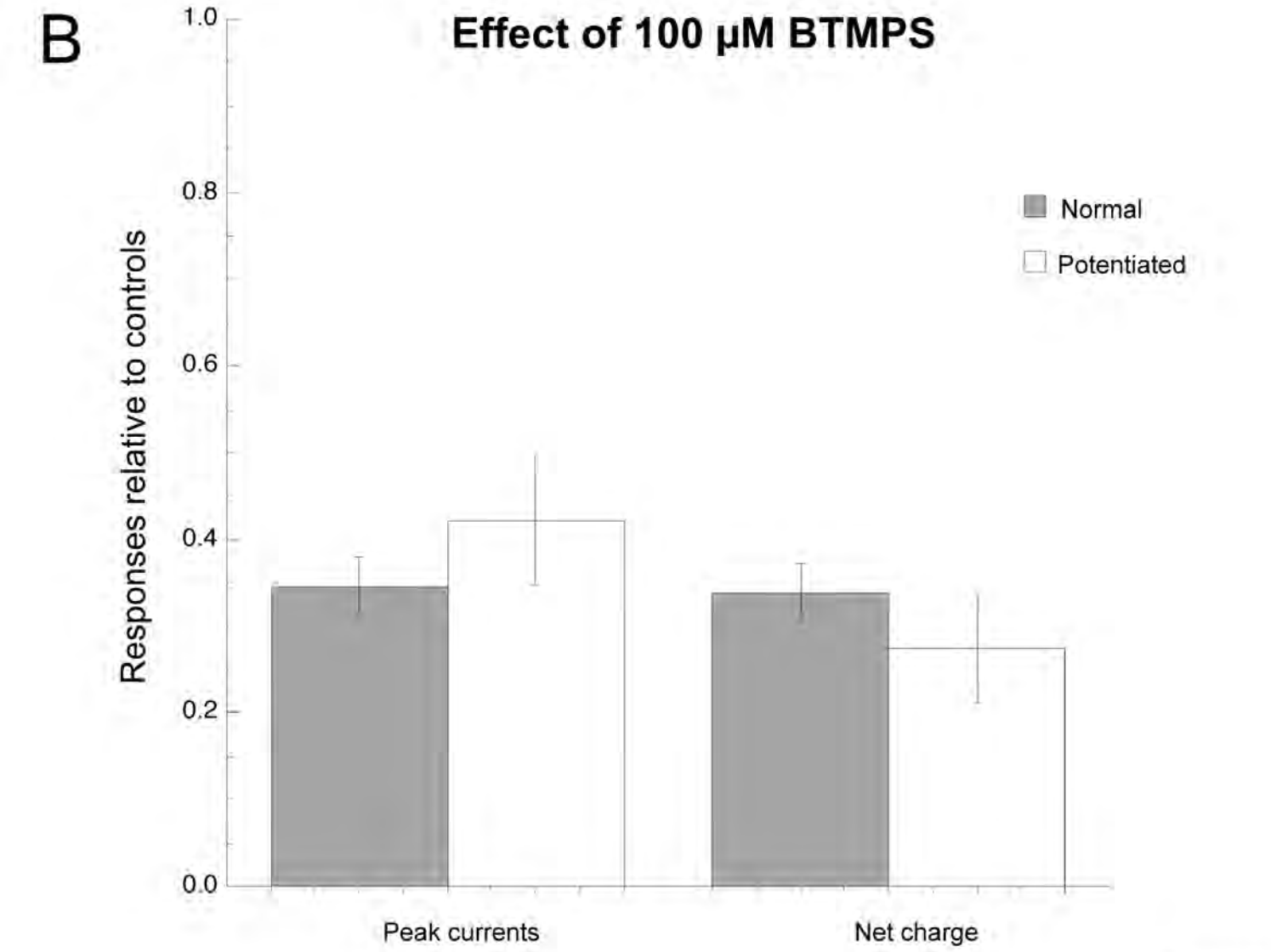
B
Effect of 100 µM BTMPS
Responses relative to controls
1.0
0.8
0.6
0.4
0.2
0.0
Normal
Potentiated
Peak currents
Net charge

Figure 3

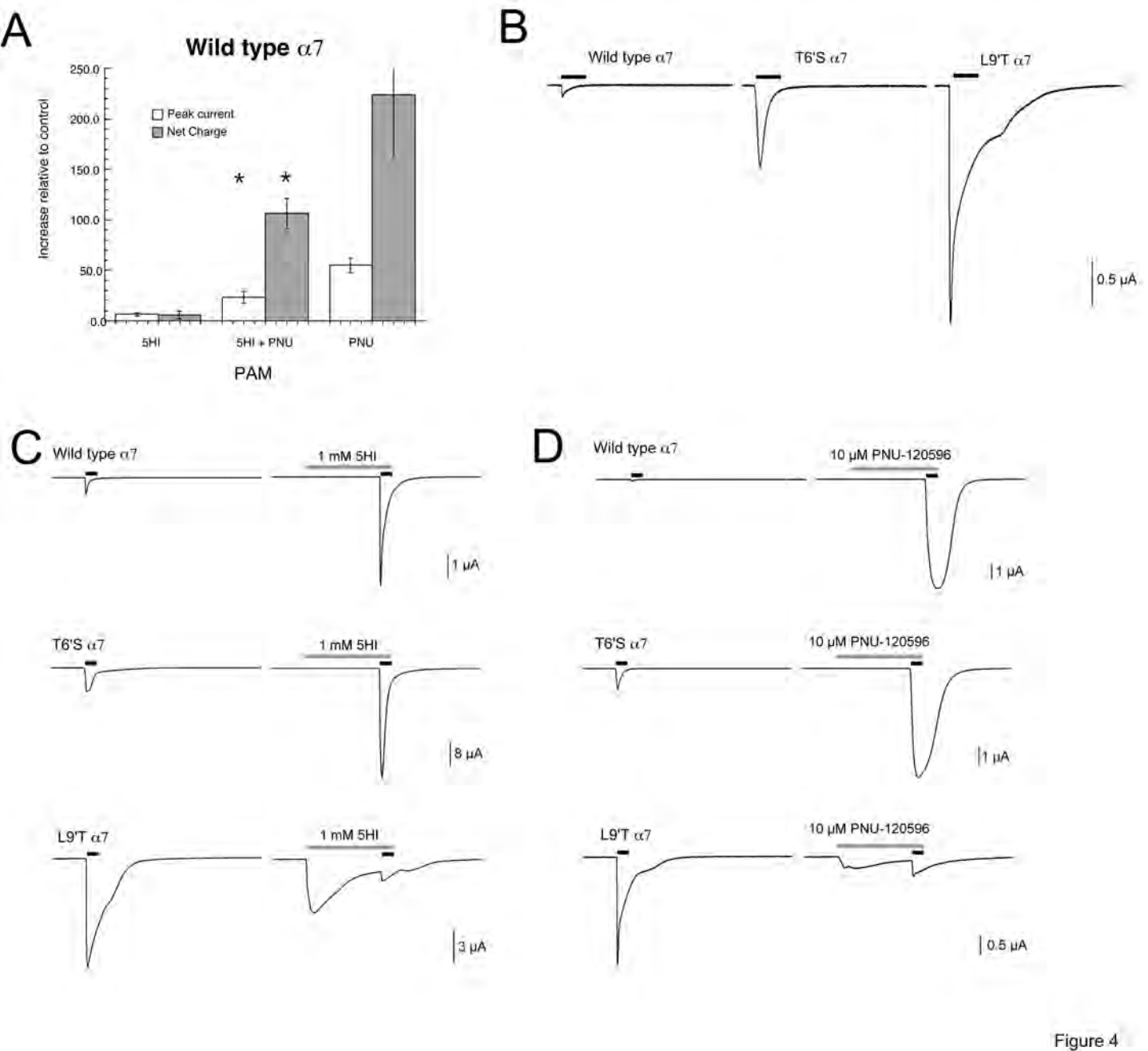
A
Wild type α7
Increase relative to control
250.0
200.0
150.0
100.0
50.0
0.0
Peak current
Net Charge
*
*
5HI
5HI + PNU
PNU
PAM
B
Wild type α7
T6'S α7
L9'T α7
0.5 μA
C
Wild type α7
1 mM 5HI
1 μA
T6'S α7
1 mM 5HI
8 μA
L9'T α7
1 mM 5HI
3 μA
D
Wild type α7
10 μM PNU-120596
1 μA
T6'S α7
10 μM PNU-120596
1 μA
L9'T α7
10 μM PNU-120596
0.5 μA

Figure 4

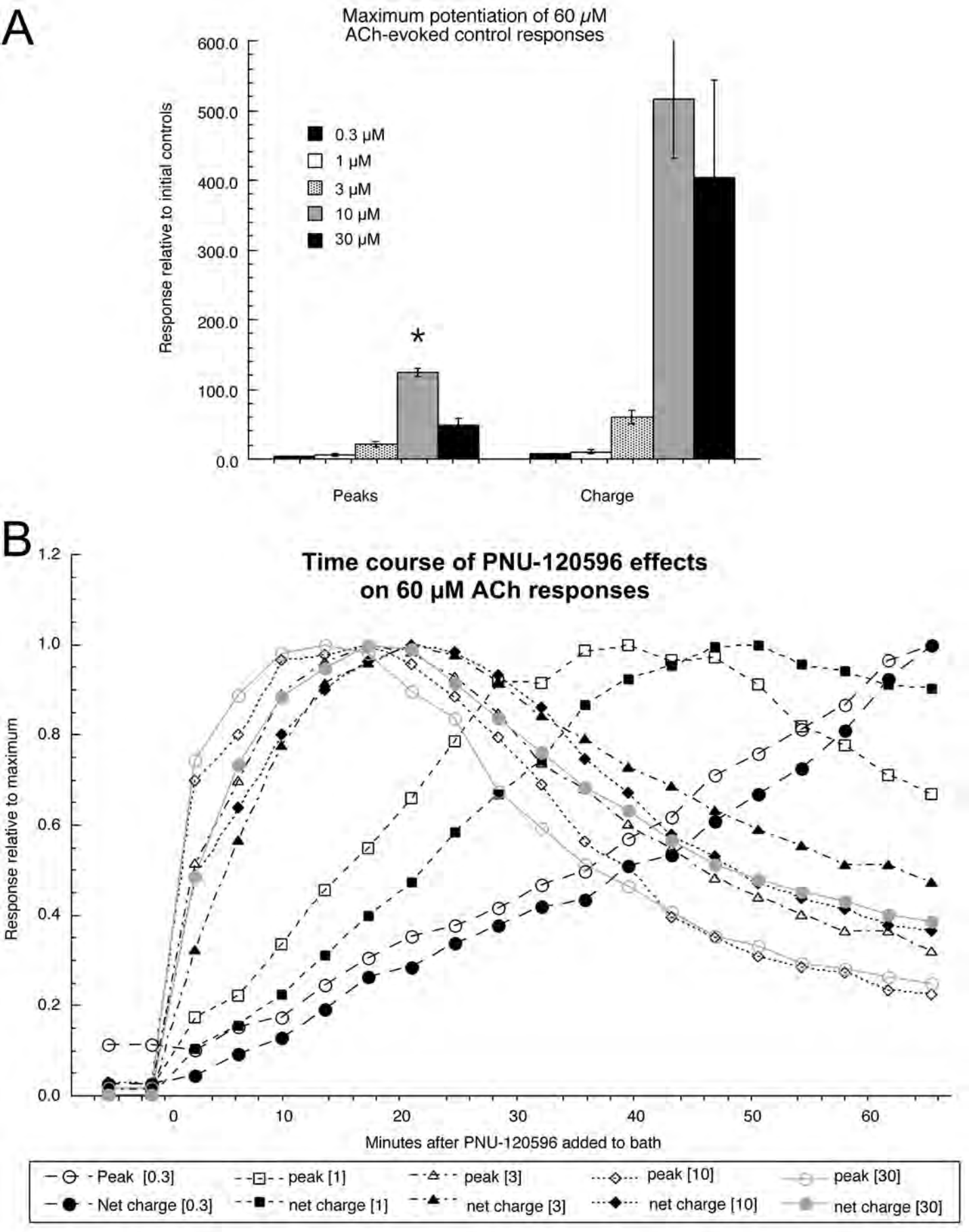
A
Maximum potentiation of 60 μM
ACh-evoked control responses
Response relative to initial controls
600.0
500.0
400.0
300.0
200.0
100.0
0.0
0.3 μM
1 μM
3 μM
10 μM
30 μM
*
Peaks
Charge
B
Time course of PNU-120596 effects
on 60 μM ACh responses
Response relative to maximum
1.2
1.0
0.8
0.6
0.4
0.2
0.0
0
10
20
30
40
50
60
Minutes after PNU-120596 added to bath
Peak [0.3]
peak [1]
peak [3]
peak [10]
peak [30]
Net charge [0.3]
net charge [1]
net charge [3]
net charge [10]
net charge [30]

Figure 5

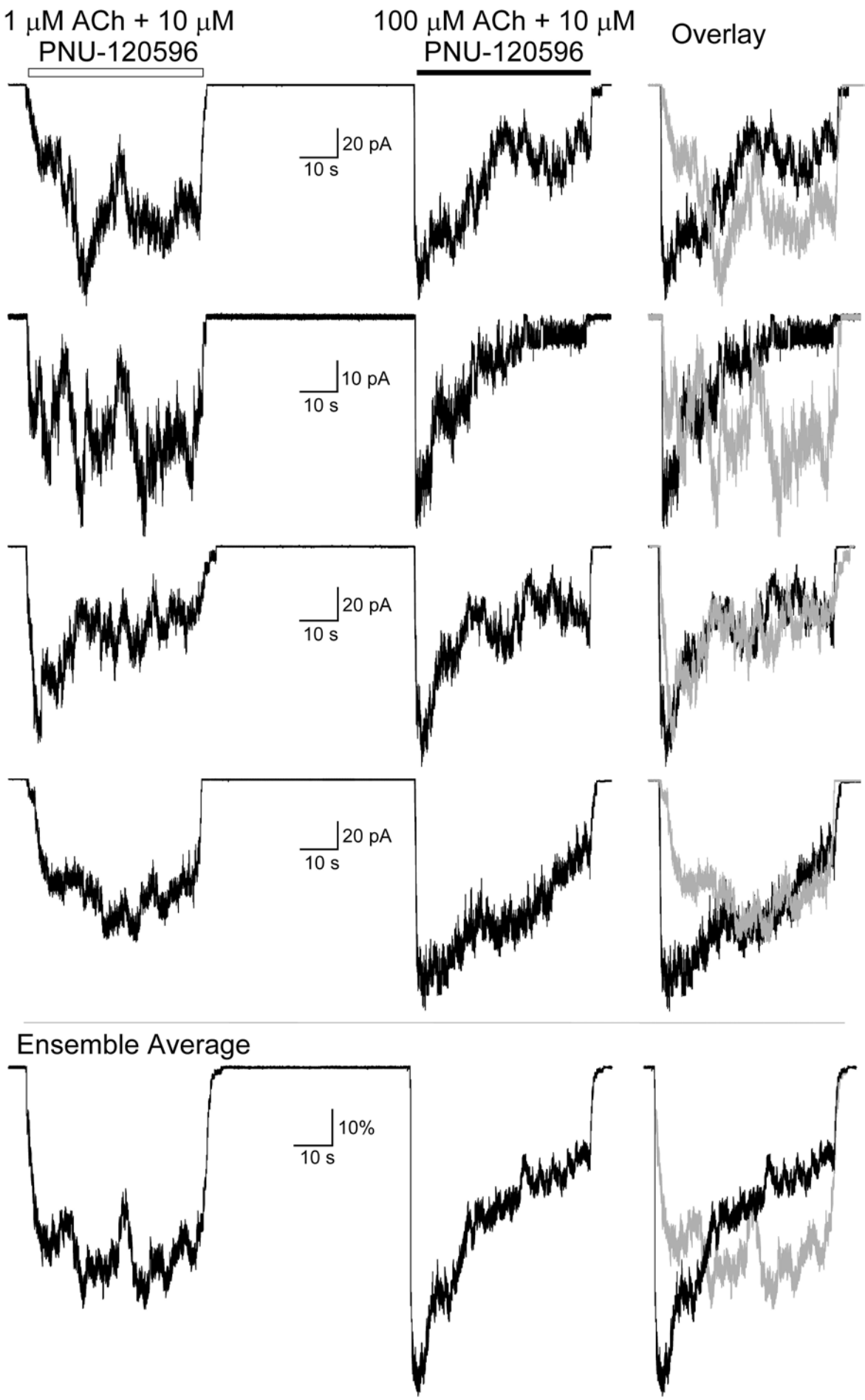
1 μM ACh + 10 μM PNU-120596
100 μM ACh + 10 μM PNU-120596
Overlay
20 pA
10 s
10 pA
10 s
20 pA
10 s
20 pA
10 s
Ensemble Average
10%
10 s

Figure 6

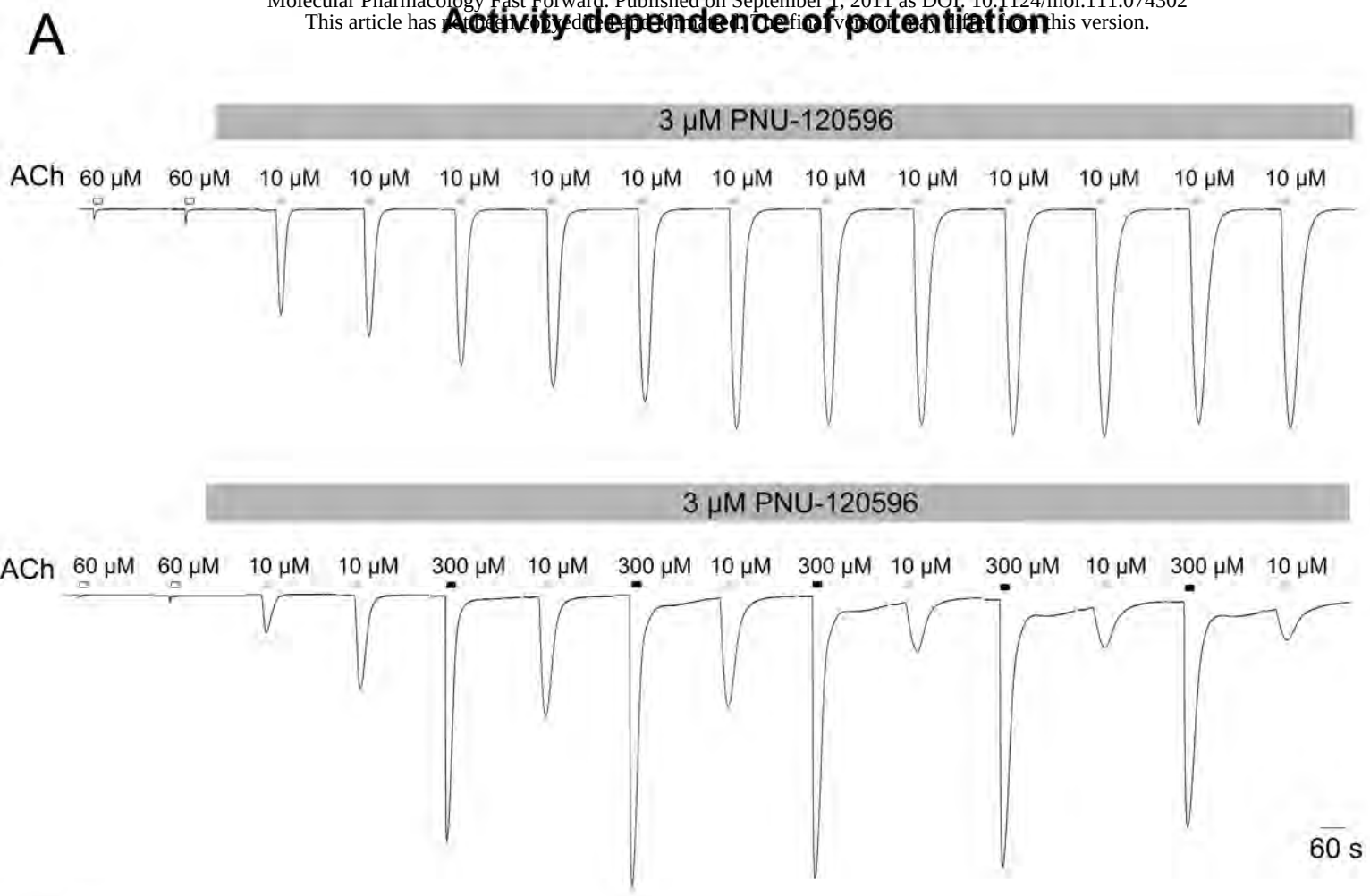

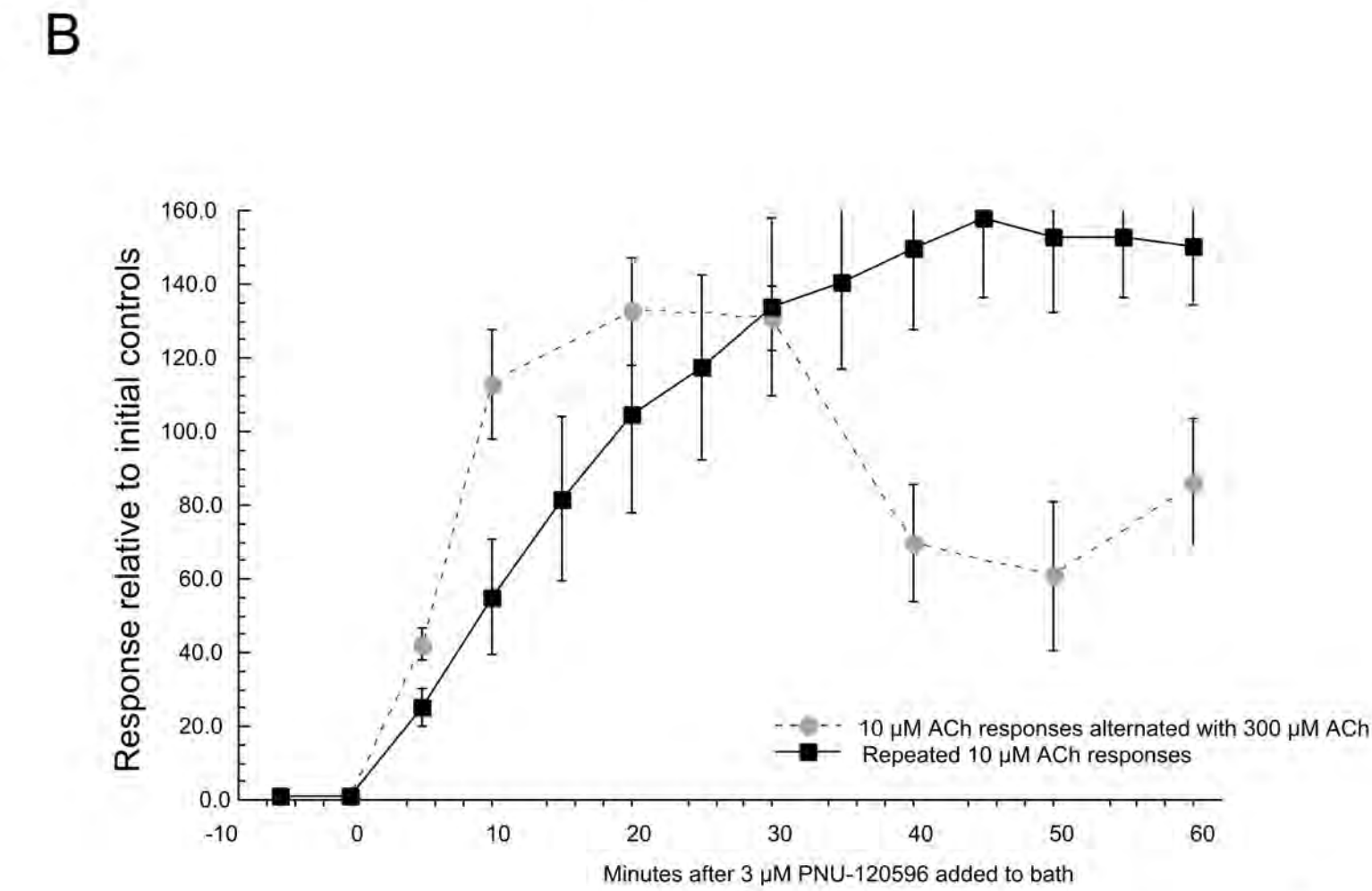

Figure 7

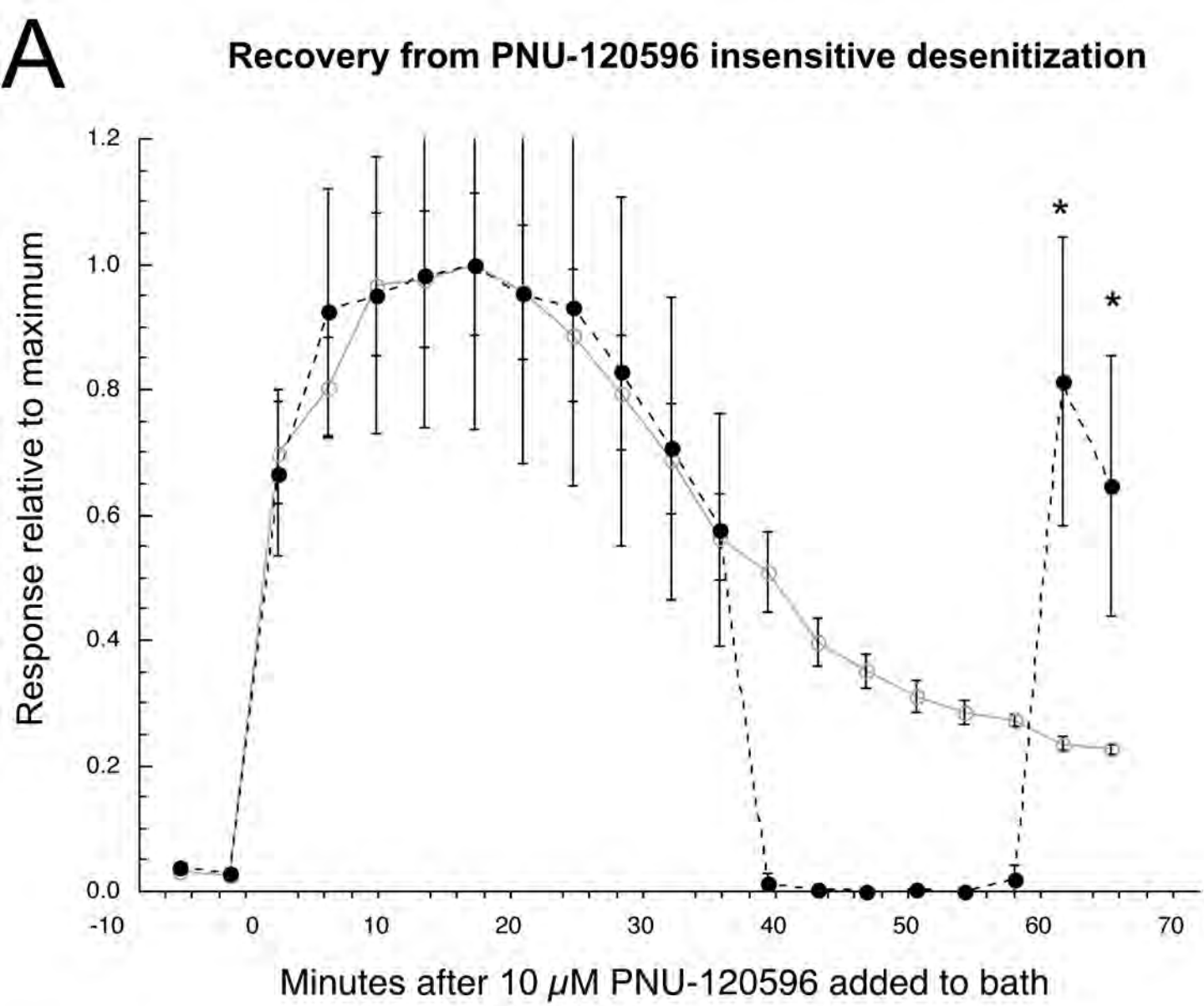
A
Recovery from PNU-120596 insensitive desenitization
Response relative to maximum
1.2
1.0
0.8
0.6
0.4
0.2
0.0
-10
0
10
20
30
40
50
60
70
*
*
Minutes after 10 μM PNU-120596 added to bath

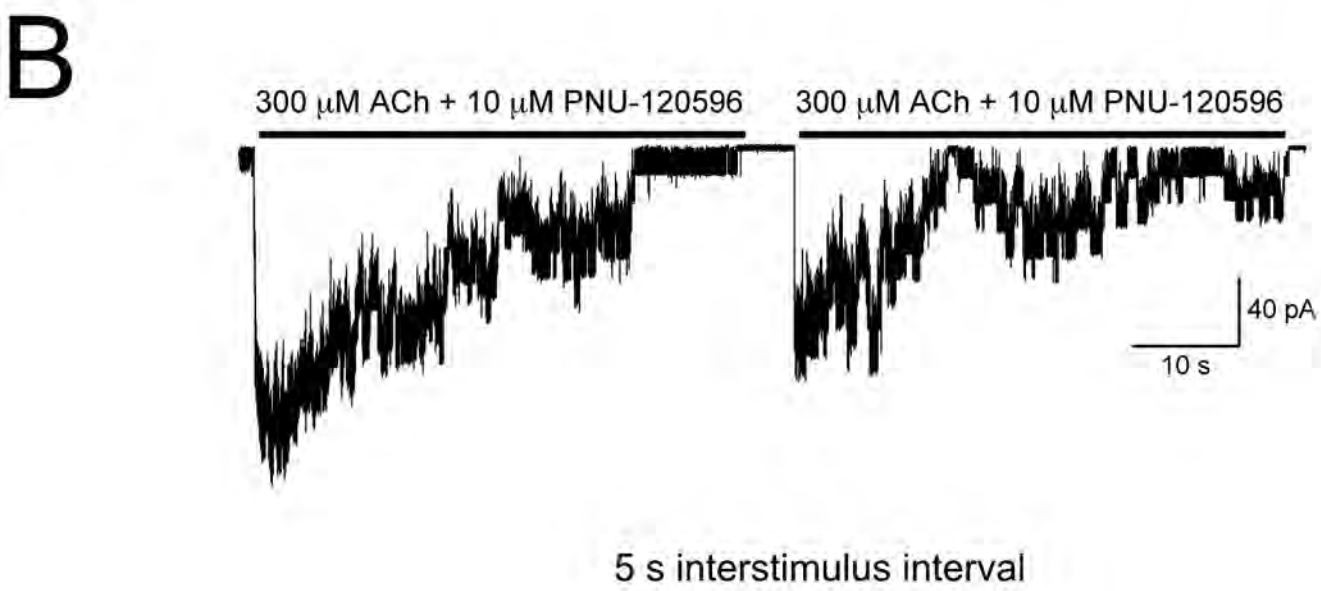
B
300 μM ACh + 10 μM PNU-120596
300 μM ACh + 10 μM PNU-120596
40 pA
10 s
5 s interstimulus interval

Figure 8

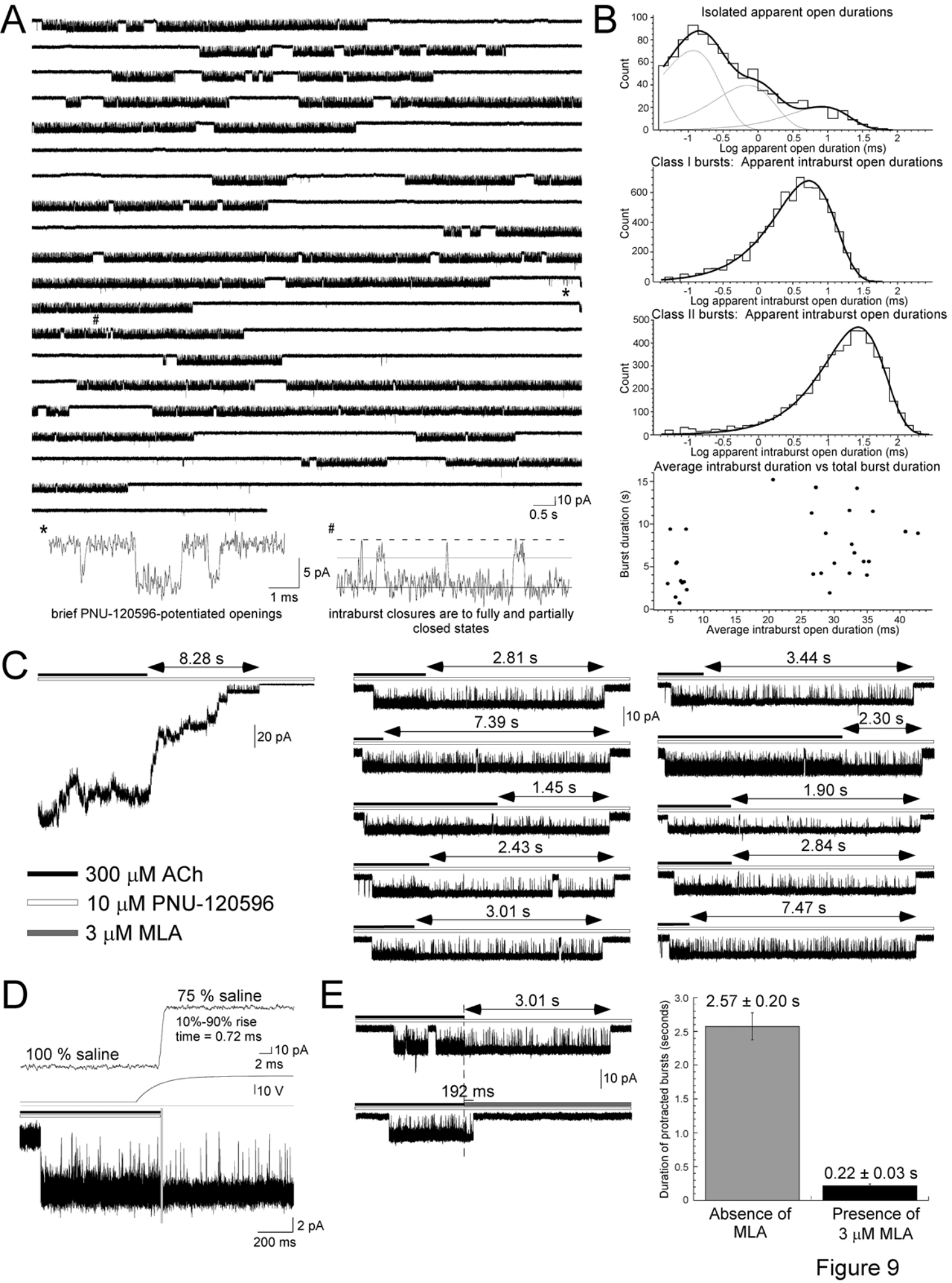
A
10 pA
0.5 s
*
#
5 pA
1 ms
brief PNU-120596-potentiated openings
intraburst closures are to fully and partially closed states
B
Isolated apparent open durations
Count
Log apparent open duration (ms)
Class I bursts: Apparent intraburst open durations
Log apparent intraburst open duration (ms)
Class II bursts: Apparent intraburst open durations
Average intraburst duration vs total burst duration
Burst duration (s)
Average intraburst open duration (ms)
C
8.28 s
20 pA
2.81 s
7.39 s
1.45 s
2.43 s
3.01 s
3.44 s
2.30 s
1.90 s
2.84 s
7.47 s
10 pA
300 μM ACh
10 μM PNU-120596
3 μM MLA
D
75 % saline
10%-90% rise
time = 0.72 ms
100 % saline
10 pA
2 ms
10 V
2 pA
200 ms
E
3.01 s
10 pA
192 ms
2.57 ± 0.20 s
0.22 ± 0.03 s
Duration of protracted bursts (seconds)
Absence of MLA
Presence of 3 μM MLA

Figure 9

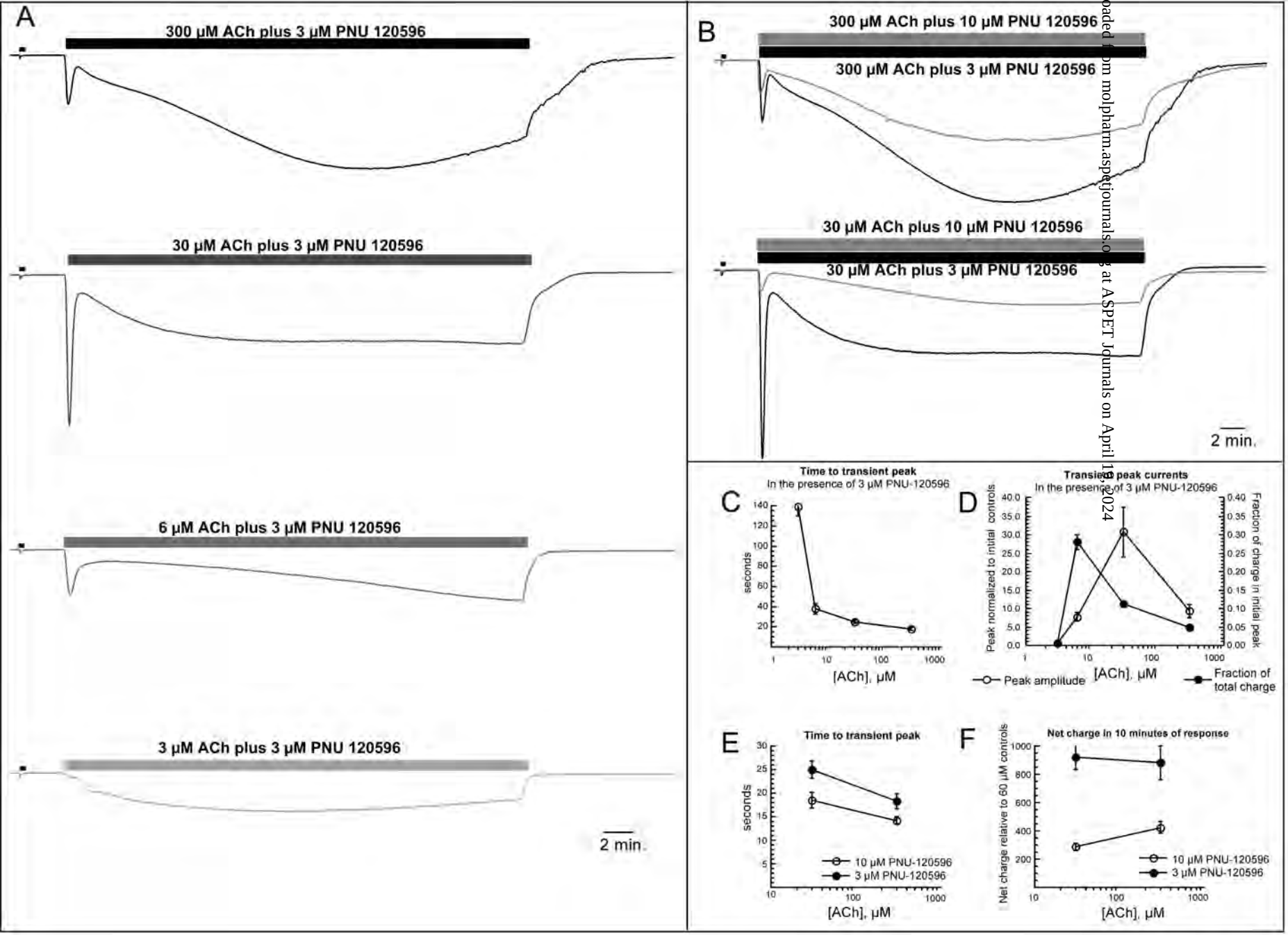

Figure 10

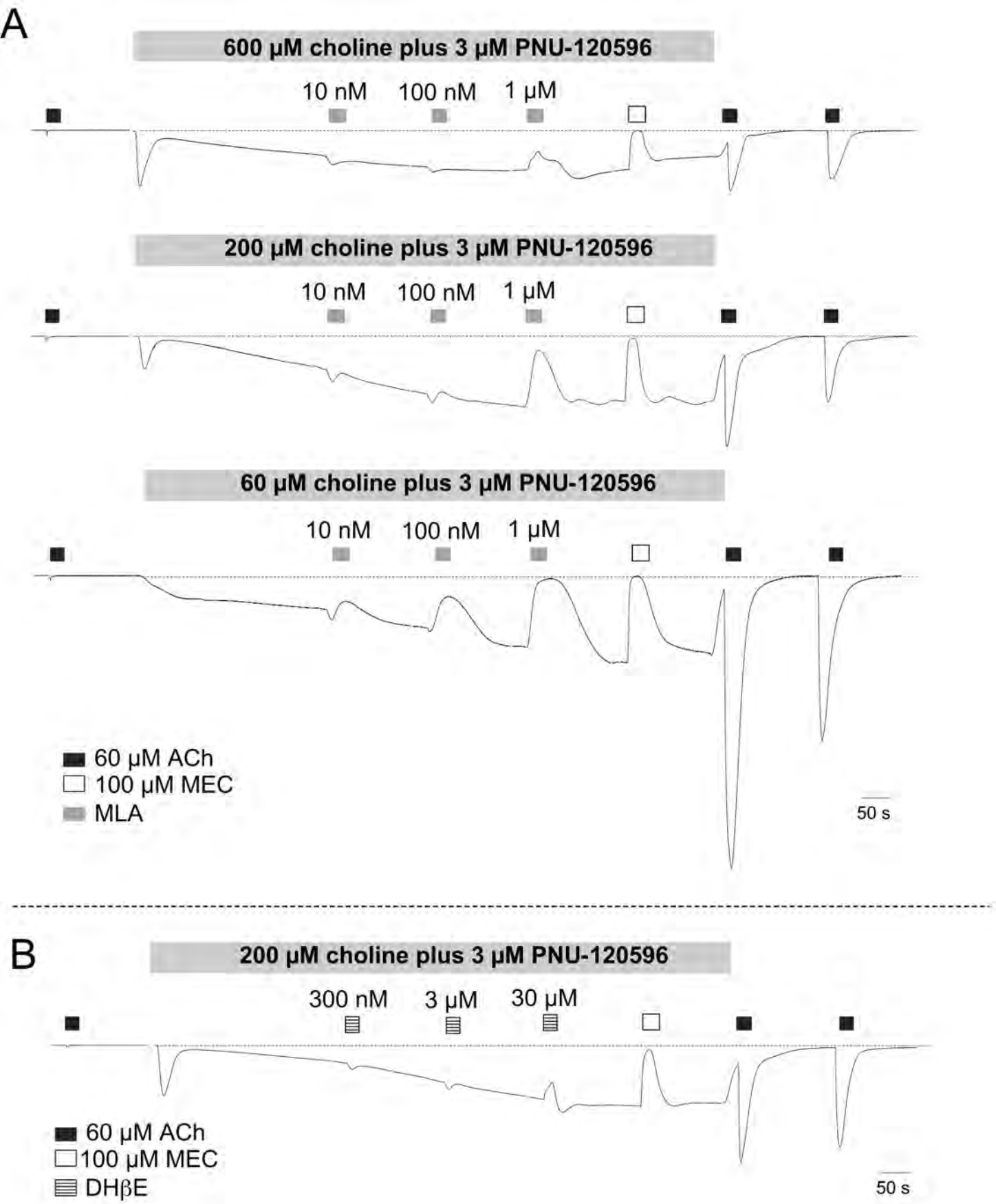
A
600 µM choline plus 3 µM PNU-120596
10 nM
100 nM
1 µM
200 µM choline plus 3 µM PNU-120596
10 nM
100 nM
1 µM
60 µM choline plus 3 µM PNU-120596
10 nM
100 nM
1 µM
60 µM ACh
100 µM MEC
MLA
50 s
B
200 µM choline plus 3 µM PNU-120596
300 nM
3 µM
30 µM
60 µM ACh
100 µM MEC
DHβE
50 s

Figure 11

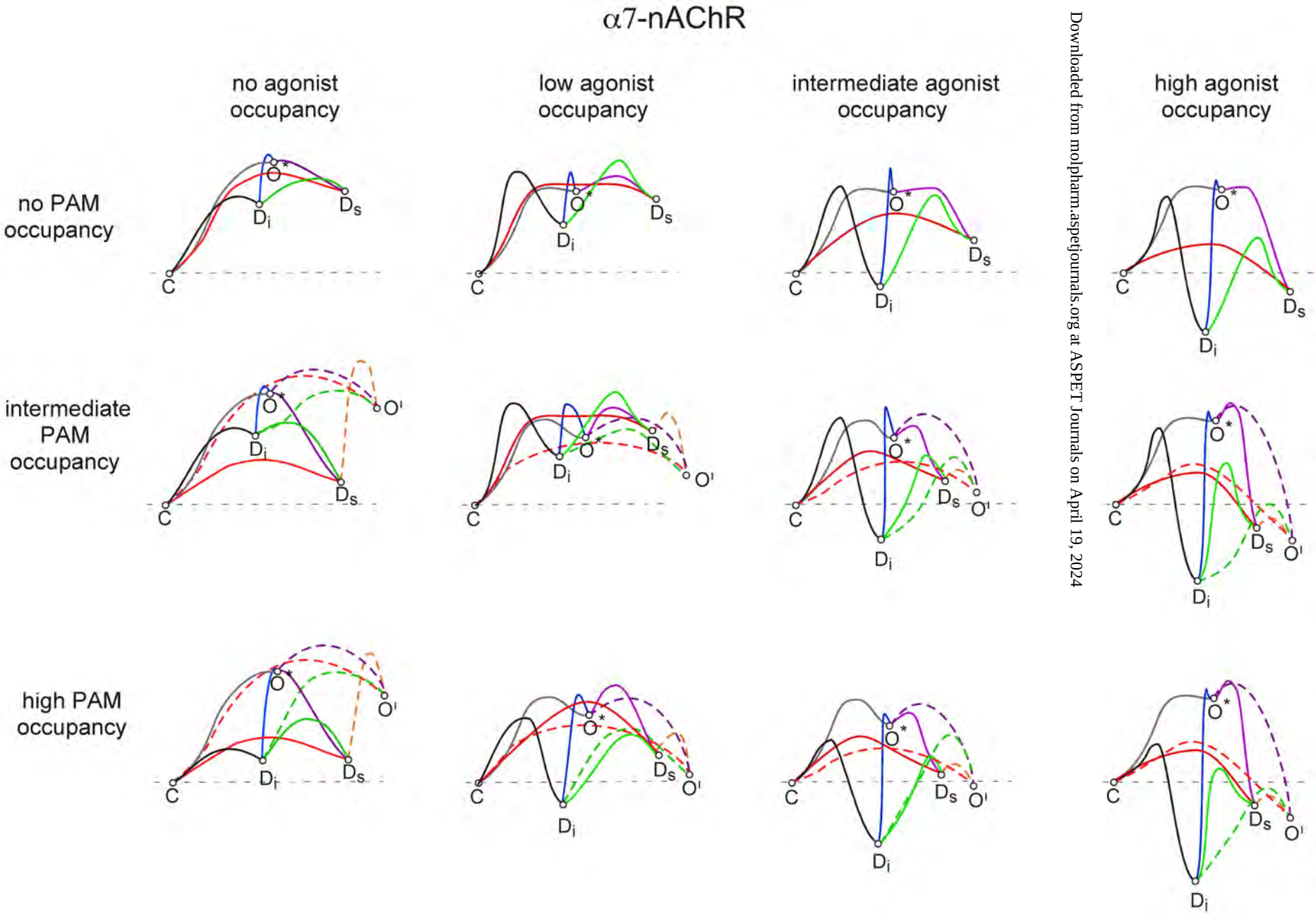

Figure 12